# FIRE ANALYSIS OF CAR PARK BUILDING STRUCTURES

**Bilal Fettah**

Final thesis presented to the

**School of Technology and Management**

**Polytechnic Institute of Bragança**

**for the fulfilment of the requirements for a Master's Degree in**

**Industrial Engineering**

(Mechanical Engineering branch)

**July 2016**

This page was intentionally left in blank

# FIRE ANALYSIS OF CAR PARK BUILDING STRUCTURES

**Bilal Fettah**

Master Thesis Presented To

**School of Technology and Management**

**Polytechnic Institute of Bragança**

to the fulfilment of the requirements for a master's degree in

## Industrial Engineering

Supervisor at IPB: Prof. Dr. Paulo Piloto

Supervisor at UHBC: Prof. Dr. Abdallah Benarous

**July 2016**

This page was intentionally left in blank

**ACKNOWLEDGEMENT**

I would like to express my gratitude and appreciation to Professors Paulo Piloto and Abdallah Benarous for their excellent guidance, supervision, dedication and support throughout the year I have spent working with him; their experience in the field of structural fire engineering has also been a precious source of inspiration. The advices and comments of both professors that have been a considerable help and of great value for the successful and conclusion of this work.

A special thanks goes to my family and friends for their continuous support, patience and for agreeing to let me live far from Algeria for this Erasmus + ICM, Intership and double diploma award between the Polytechnic Institute of Bragança (IPB) and the University Hassiba ben Bouali de Chlef (UHBC).

Thank you for your helpful technical advice, your support and encouragement during this period, for your cheerfulness, patience and love; thank you for always being at my side.

Finally, all the thanks to Allah for give me the energy and the motivation to complete this thesis with your beautiful smiles.

This page was intentionally left in blank

**ABSTRACT**

The thermal loading of an open car park building structure is going to be analysed, based on different fire scenarios that depend on the type of vehicle (different heat release rate). The compartment is going to be fixed and the thermal effect on beams is going to be analysed, depending on the vehicle position. The result of simple calculation method will be used to determine several temperature-time curves. The simple calculation method (Hasemi method) is also to be compared with the calculations of the Elefir-EN calculation program to analyse the thermal effect of the localized fire on beams.

**KEY-WORDS:** Localized fire; Open Car park; Steel structure; Elefir-EN, correlative models.

This page was intentionally left in blank

**RESUMO**

A carga térmica uma estrutura de um parque de estacionamento aberto será analisada, tendo em consideração diferentes cenários de incêndio que dependem do tipo de veículo considerado (diferentes taxas de libertação de calor). O compartimento em estudo será fixo e o efeito térmico do incêndio nas vigas será analisado em função da posição do veículo. Os resultados do método simplificado de cálculo serão utilizados para determinar as curvas de evolução de temperatura-tempo. O método de cálculo simplificado (Hasemi) é também comparado com o resultado do programa elefir-EN, sendo analisado o efeito térmico do incêndio localizado nas vigas.

**PALAVRAS CHAVE:** Incêndio localizado, Parque de Estacionamento Aberto, Estrutura em Aço, modelos de correlação.

This page was intentionally left in blank

**INDEX**

## INDEX OF FIGURES

## INDEX OF TABLE

## ABBREVIATIONS LIST

### Constants

| | | |
|---|---|---|
| $g$ | Gravitation acceleration | [9.81 m/s$^2$] |
| $\alpha_c$ | Convection heat transfer coefficient | [25 J/m$^2$ K] |
| $\Phi$ | Stephan Boltzmann constant | [5.67×10$^{-8}$ W/m$^2$K$^4$] |

### Variables

| | | |
|---|---|---|
| $\varepsilon_m$ | Emissivity of the surface material | [-] |
| $\varepsilon_f$ | Emissivity of the fire | [-] |
| $\sigma$ | Shape factor | [-] |
| $k_{sh}$ | Correction factor | [-] |
| $\varepsilon$ | Rate of dissipation of turbulent energy $k$ | [m$^2$/s$^3$] |
| $L_f$ | Flame Length | [m] |
| $\theta_{(z)}$ | Temperature in vertical flame axis | [°C] |
| $D$ | Diameter of the fire | [m] |
| $Q$ | Heat Release Rate | [W] |
| $Q_c$ | Convective part of the heat release Rate | [W] |
| $Z$ | High along the flame axis | [m] |
| $H$ | Distance between the fire source and the ceiling | [m] |
| $Z_0$ | Virtual origin of the fire axis | [m] |
| $H_a$ | Height of the lower flange from the floor | [m] |
| $r$ | Distance between fire axis and the beam section | [m] |
| $L_H$ | Horizontal length of the flame | [m] |
| $H_s$ | Vertical position of the fire source | [m] |
| $Q_H^*$ | The non-dimensional heat release rate | [-] |
| $Q_D^*$ | The non-dimensional heat release rate | [-] |
| $\dot{h}$ | The heat flux | [kW/m$^2$] |
| $y$ | Non dimension parameter | [-] |
| $T$ | Surface temperature of material | [°C] |
| $\theta$ | Local temperature of gas | [°C] |
| $\dot{h}_{net}$ | The heat net flux | [kW/m$^2$] |
| $T_{gas}$ | Gas temperature | [°C] |
| $T_{steel}$ | Steel temperature | [°C] |
| $C_a$ | Specific heat of steel | [J/kg°C] |
| $\lambda_a$ | Thermal conductivity | [W/m K] |
| $\Delta t$ | Time variation interval | [s] |
| $\Delta T_{steel}$ | Increase of steel temperature at the time t | [°C] |
| $A_m/V$ | Section factor of steel profile | [m$^{-1}$] |
| $A_m$ | Surface area of the steel member | [m$^2$] |
| $V$ | Volume of the steel member | [m$^3$] |

# CHAPTER 1: INTRODUCTION

## 1.1- Background

The increase of the market shares for steel and composite car parks in Europe is somewhat limited by the lack of information on how these structures behave under exceptional localised fire. Nowadays, in European countries most of these car parks are built above the ground because of a lower price per parking place, lower energy consumption, use of natural light and natural ventilation.

Previous or ongoing relevant projects are presented, relative to car fire tests and car park fire tests requirements for robustness, ductile joints, structural safety. Statistics about real fires in open car parks show that car fires have never been dangerous neither for the stability of the structure nor for the people. The fire normally stays local and the maximum number of cars involved in a fire are three cars. It results that most unprotected steel in open sided steel-framed car parks has sufficient inherent resistance to withstand the effects of any fires that are likely to occur.

The development of a localised car fire in a car park can be studied according to fire scenarios. In France, three basic scenarios were defined by the CTICM [1] to design car park structures submitted to fire, including up to seven cars in a fire. The Heat Release Rate (HRR) curves were obtained from previous research works for different vehicle types. References to HRR curves obtained by the CTICM tests in [2] for a single class 3-car fire and three class 3-cars with a fire propagation time of 12 minutes are specially detailed in this report.

The structural behaviour of the building can be studied by specific combinations for mechanical and thermal loadings in the open car park structure, defined by EN 1991-1-2:2002 [3]. The EN1993-1-2:2005 [4] defines the rules to calculate the fire resistance of any steel structural element in open car parks. The net heat flux to structural elements from each car fire is a function of the position, the height of the ceiling, the diameter of the fire source, the HRR and the distance from the element to the fire (radial position).

Steel and concrete are the most commonly used materials for open car parking with unprotected steel or composite steel-concrete structures is a solution frequently used in many countries of the centre and north of Europe, or even in United-States, Canada or Japan. There are many advantages of a composite steel-concrete structure for open car park buildings: I) shorter on-site construction schedule due to the prefabricated elements, and consequently lower construction cost, as well as lower environmental impacts during construction; ii) flexible

column spacing up to around 16 m, allowing to locate the columns at the back of the parking bay which facilitates vehicles manoeuvres, iii) reduced column section size in comparison to a concrete structure, which increases the parking spaces; and iv) reduced weight, and smaller foundations, in comparison to concrete structures [5].

Recent major events have caught world attention on safety and have raised public awareness worldwide. Several safety critical events are possible to occur: fires, explosions, toxic releases, losses of hazardous goods, and such accidents could take place in industrial plants as well as in large public buildings (skyscrapers, offices, hotels, malls, warehouses, museums, concert halls, train and metro stations, road and railway tunnels).

Vehicle parking buildings are commonly found in most modern urban environments. Such buildings can be stand-alone structures or attached to other occupancy types. The buildings can be multi-storey; above ground or below ground; be fully or partially enclosed; and be used to park a range of vehicle types (cars, vans, buses etc.). The usage characteristics of such buildings will depend on the service they provide: parking for patrons of a shopping mall, long-stay parking at an airport, parking for the residents of household units etc. This particular research is focused on car parking buildings rather than for other vehicle types such as trucks or buses and the approach is similar to previous vehicle-fire related research [6], such that fire risk is equal to probability multiplied by consequence.

Field modelling based on the Computational Fluid Dynamics methodology plays a very important role in fire research. With the fast growth of computer technology and the progress in CFD technology and theory, field models are becoming a common engineering practice in the fire safety design and hazard assessment of buildings, and would ultimately be the most satisfactory treatment for fire safety research in buildings and enclosures.

For the systematic design of an effective fire detection, protection and smoke control system, it is essential that these fundamental transport processes are properly understood and that the key components (smoke and toxic gases spread, temperature distributions, the velocity field) are clearly identified and accurately predicted. CFD codes can potentially be used to evaluate the effects of changes in structural design and in emergency ventilation systems, and to assess performance of safety measures over a range of fires, differing in size, duration and locations [7]. CFD modelling is common in the context of Fire Engineering Ph.D. Research activities, [8]. The author in this document just discussed the issue of numerical modelling as a practical aid for the development of smoke control strategies in buildings and addressed the simulation of combustion and fire-induced flows in enclosures by using the JASMINE code.

The author obtained predictions within 30% of the measurements, and highlighted the need of more well-defined experiments for CFD model comparisons.

Regarding tunnel fires simulations, Bakar [9] used Fluent for a study of the effect of tunnel aspect ratio on control of smoke flow in tunnel fires. This author carried out both experimental tests and CFD simulations, with the overall flows in the tunnels well reproduced. Nevertheless, the predicted velocity was slightly lower than the experimentally measured one, and the simulations also failed to give good temperature predictions near the fire region.

The FDS code was employed by Pope [10] for CFD modelling of large-scale compartment fires. Among his most interesting findings, this author underlined the sensitive dependence on initial and boundary conditions in CFD simulations, a rarely addressed result in the published literature.

Hart [11] was involved in numerical modelling of tunnel fires and water mist suppression: a series of CFD simulations by Fluent code were used to successfully apply the Lagrangian particle-based model to the simulation of water mist systems for fire suppression, both in an enclosure (with the results consistent with experimental data) and in a tunnel. The behaviour of the mist was shown to be intimately linked with both the ventilation air flow and the fire induced flow. However, owing to the very long required run time CFD modelling is not yet practical for routine design of water mist systems.

### 1.2- Aim of The Work

On the basis of the above described background, the aim of this thesis was to perform a Fire Analysis of open car park building structure under fire by and using the simplify calculation method (Heskestad, Hasemi) to be compared with Elefir-EN calculation software [12]

The thesis presents a methodology for assessing the structural behaviour parking lots open metal structure (or mixed steel-concrete), in case of fire. This methodology is characterized by the following steps [13]: (i) setting set of fire, (ii) calculating the heat release rate, (iii) analysing the structural behaviour.

The objectives of this study were i) to present the design method of an open car park based on fire scenarios, ii) apply the design methodology to an open parking made by steel and concrete using the Elefir-EN calculation program [12]. The program allows to easily calculate the fire resistance of simple metal elements subjected to any mechanical and thermal load. For localized fire, the program determines, according to the diameter of the fire and free ride height

if the flame touches the ceiling or not, and then calculates the temperature of the elements (primary/secondary beams or columns).

### 1.3- Outline of The Thesis

The thesis is divided into six chapters. In the first chapter, a global overview of the unprotected steel in open car park under fire and with a concrete slab is described, and the objectives and organization of the research are drawn. The second chapter provides a general idea about some fire events in open car park buildings in the world and the Fire requirements in different European countries under localised fire observed in real fire tests to the verification and design rules. Chapter three describes and discuss the experimental result for different models of burning car, according to the different classification the heat release rate (HRR) as a result of the investigation from the ECCS Project, and in order to define some fire scenarios, a typical car park structure was chosen. It corresponds to the car park structure designed according to European standards. Chapter four describe the method of analysis of the structure (open car park) using the annex c of Eurocode 1991-1-2 [3] and with the iterative procedure of the non-linear equation solution of the newton Raphson method, according to the net heat flux at the boundaries of a steel profile, taking into account the flux lost due to the temperature of the section we calculate the temperature evolution of the unprotected steel (beams) according to the Hasemi and Heskestad models. The chapter five presents a comparison of the result obtain by the software Elefir-EN, the temperature versus time curves for to model the thermal response of the steel beams of an open car park subjected to a localized fire according to annex C of part 1-2 of Eurocode 1. Finally summarizes the main conclusion of the work in terms of recommended improvements in open car park safety.

# CHAPTER 2: OPEN CAR PARK FIRES

## 2.1- Historic Events

### 2.1.1- Car Park Fires

A short list is given for reported damages in real car park fire accidents that occurred mostly in the Netherlands during the period 2002–2007.

#### 2.1.1.1- Schiphol Airport (The Netherlands)

In October -2002 in a car park near Schiphol airport a fire took place. Around 30 cars were involved on fire at the same time. Also the fire spread was much faster than currently assumed. The fire occurred in a car park of a car rental company, which led to some specific circumstances that might have caused the more rapid fire spread than normally expected [14].

The structure consisted of massive pre-tensioned concrete slabs which are supported by concrete T-girders. It was a very large fire, because the car park was fully booked, with only 40cm spacing between the cars. See the Figure 1.

Figure 1: Picture after the fire in the car park near Schiphol airport. [15]

Furthermore, all cars were parked on a small distance of each other, which can enhance fire spread from car to car and All cars were new and new cars contain more plastic parts than older cars. Plastics can be ignited more easily and produce more Heat Release Rate.

All fuel tanks of the cars were completely filled, leading to a high fire load and the fuel tanks were made of plastic and started leaking fuel, creating pool fires which can also cause spreading of fire, by draining away under other cars.

#### 2.1.1.2- Apartment building Geleen (The Netherlands)

During the night of 23–24 of June 2004 a fire happened in a car park beneath an apartment building in Geleen. Twelve vehicles burned in total. The concrete was heavily damaged with complete cover loss for the slabs, walls and some columns. The structure was repaired with shotcrete and supplementary reinforcement [14].

The parking garage is about 21.5 m width and 15 m deep. The parking garage consists of a partial covering of the courtyard used for parking cars. On the front side, the garage is fully open, the walls consist of reinforced concrete and the construction of the ground floor is a large slab floor. The total thickness of the walls is 250 mm. On the underside of the floor a 100 mm fiber board is provided for the purpose of thermal insulation.


Figure 2: The Geleen car park after the fire. [15]

The fire was probably started in the back of the garage, during the fire, a total of 12 cars were involved. Due to the heavy smoke, residents had to be evacuated from the building. Considerable damage was detected after the fire so that the building was not used for some time. As a result of the fire, the fibre boards were locally attached against the ceiling and concrete has fallen by spalling [16]. Also, the walls and a number of columns presents spalling of concrete. Figure 2 shows failure of concrete cover and the rehabilitation of the ceiling.

#### 2.1.1.3- Gretzenbach (Switzerland)

A fire took place on November 11, 2004, in a car park in Gretzenbach. After approximately 90 min, the roof of the underground car park collapsed due to punching and 7 firemen died during their intervention. Fire investigation revealed design and execution mistakes resulting in an overload of soil and a decreased punching shear capacity. Because of the occurrence of a clear punching failure and the typical car park geometry, this example is used as the basis for the geometry of the case study presented in [14].


Figure 3: Gretzenbach underground car parking 2004. [17]

#### 2.1.1.4- Apartment building Harbour Edge (The Netherlands)

A fire occurred on October 1, 2007, in the open car park of an apartment building (Harbour Edge) in Rotterdam. The twelve storey building is predominantly in use for housing and for business companies and was completed in 2007. The lower part of the building contains a two storey of open car park. The building is presented in Figure 4.

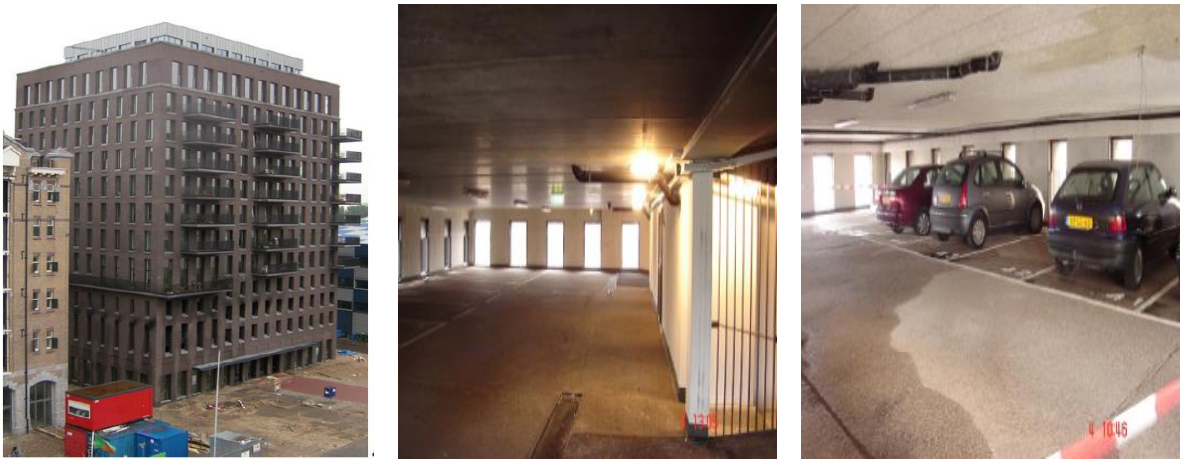

Figure 4: The building 'Harbour Edge' in Rotterdam Netherlands. [17]

The building is primarily a concrete structure with a pile foundation. At the fire location the load bearing structure of the floors consists of hollow core slabs with a height of 260 mm, and on top of it there is a compression layer with a varying thickness of some 70 to 90 mm. The hollow core slabs have a span distance of approximately 11 m and the concrete cover on the pre-stressing strands is approximately 40 mm. These hollow core slabs are supported on steel L-section that are fixed to the precast concrete building façade, see Figure 5.

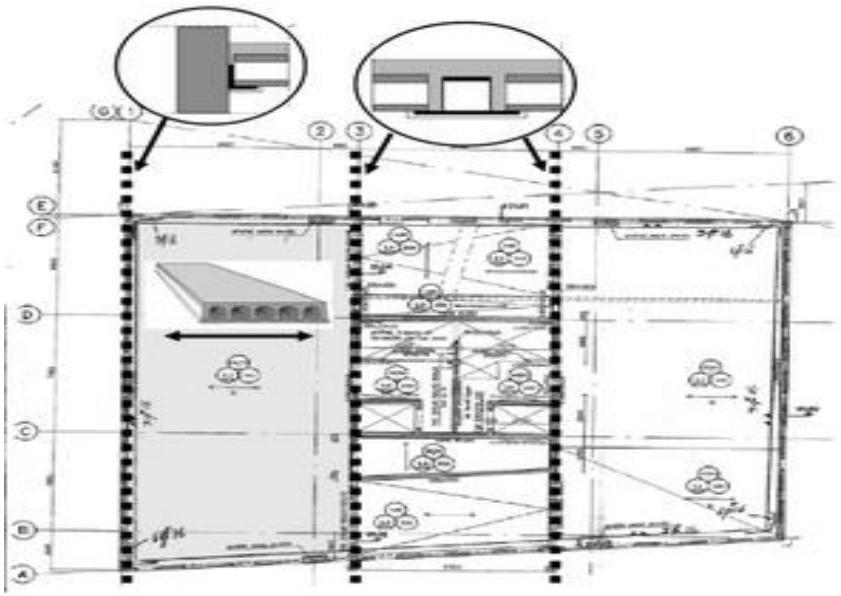

Figure 5: Overview of the structure Harbour Edge in car park. [18]

The floor is supported by steel L-section that are fixed to the walls of the concrete building core, and THQ-beams that span from the core to the façade. All exposed steel flanges are fire protected.

At the moment of the fire, 7 cars were parked at the level where the fire took place. The fire started near the middle of the first six cars parked side by side. The fire spread to both sides in this row of cars (two options are shown in Figure 6). According to Feijter and Breunese [19], it is most likely that the initial fire spread to the second car after 10 min and to the third car after 12 min. After 22 min of fire also the 4th car got involved. The moments of ignition of the 5$^{th}$ and the 6$^{th}$ car are somewhat uncertain. Finally, the 7$^{th}$ car, which was separated from the group of 6 by an empty space and which was only partially involved in the fire, was not considered to contribute to the fire in terms of HRR in the fire scenario analyses, because it was only damaged, not burnt out.

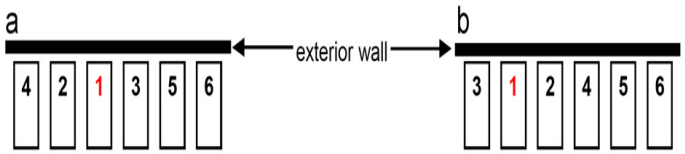


Figure 6: Possible fire sequences for the Harbour Edge fire scenario. [14]

During the fire, the fire brigade had to withdraw because of the noise of concrete falling down from the ceiling. Their impression was that parts of the hollow core slabs were collapsing. After extinguishing of the fire it appeared that six hollow core slabs had cracked horizontally through the webs, separating the slabs in an upper and lower half (compressing the pre-stressing strands). After extinguishing it was observed that four slabs had completely collapsed, as a consequence of these cracks. In the hours after the fire two more slabs collapsed.

Figure 7 : Collapsed bottom halves of hollow core slabs of the building Harbour Edge. [17]

Based on the damage pattern and observations from fire brigade and eyewitnesses, the fire development has been reconstructed. It is assumed that the 2nd and 3rd car were ignited 10 and 12 minutes after the first car, and the 4th and 5th car were ignited 22 and 24 minutes after the first car, the heat release rate and the temperature development have been calculated using Car Park Fire, that uses the design rules for localised fires as described in Eurocode EN 1991-1-2. The calculated heat release rate and temperature development on different locations are shown in Figure 8, the temperature development is in the latter figure also compared with the ISO 834 standard fire curve in [19].

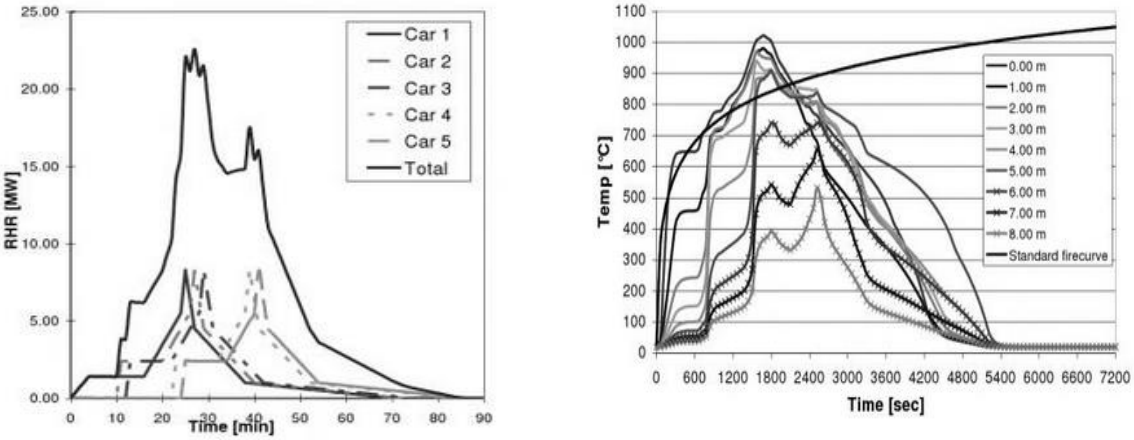


Figure 8: The HRR (left) and temperature development on different location (right). [18]

### 2.1.1.5- The Building Harbour Edge

The building Harbour Edge consists of pre-stressed hollow core slabs with a cast-in-situ concrete topping as compression layer. Additional reinforcement is provided in the compression layer as a tension ring to increase the stiffness of the slab. The load is transferred to the foundations via the facades and a central core. The design fire resistance is 120 min. A partial collapse of the structure was observed during the fire. The bottom chord of the hollow core slabs failed above the fire zone.

Even after the fire had been extinguished, during the cooling phase, further collapse of constructional elements was observed. Anchorage failure of the hollow core slabs near their support was noticed, as we as spalling of the facade. Also a horizontal cracks occurred in the concrete between the canals due to the restraint exerted by the compression layer. [17]

### 2.1.1.6- First Car Park Hilversum (The Netherlands)

On November 11, 2007, in the parking garage at Ruiterstraat Hilversum there was a fire in which two cars were involved [18]. The fire damage was limited to the superficial layers and consisted of spalling until beyond the bottom reinforcement, but only in the area of the structure directly above the fire. The parking garage is located under a residential building of two storeys. The parking garage was provided with a mechanical ventilation system. The walls of the garage consist of in situ poured solid concrete and the garage ceiling consists of a concrete slab floor.

Between the two burning cars there was a bay available under the ceiling. The concrete beam has been also damaged in the fire. Here, too, the construction of concrete was spalled. Two pictures of damage to the wide slab floor are represented in Figure 9.

Figure 9: Structural damage after the cars fire in car park at Ruiterstraat Hilversum. [13]

### 2.1.1.7- Second Car Park Hilversum (The Netherlands)

A second fire occurred on November 29, 2007 in a car park in Hilversum (the Netherlands), involving 2 cars and a motorcycle. Fire investigation revealed a maximum gas temperature about 1000 C. Nevertheless, only superficial damage could be detected on the structure [13].

## 2.2- Fire Requirements in Different European Countries

The definition of open car park can differ from country to country. ECCS (1993) [20], considers that a car park may be considered as "open" if for every parking level, the ventilation areas in the walls are situated in at least two opposite facades, equal to at least 1/3 of the total surface area of all the walls, and correspond to at least 5% of the floor area of one parking level.

Table 1 presents the limitations, the general requirements for fire ISO 834 and the indication of acceptance or not of alternative design conditions in different European countries. It is showed that in some countries, this type of building does not require (or very few) any time of fire resistance (ex.: R0 in Italy or R15 in U.K.). Portugal is one of the countries with the highest requirements for fire resistance of structural elements (from R60 to R180); however, the use of Natural Fire as an alternative to ISO fire is accepted and it is also allowed limiting or avoiding any fire protection on steel elements. This table also shows that, actually, still some of European countries prescribe long fire resistance time under ISO fire, and do not indicate anything about the use of Natural Fire (Hungary, Spain and Poland). In France and Finland, the use of bare steel is allowed if the fire safety is proved by tests or scientific studies. According to the ECCS report (1993) [20], steel structures in open car parks do not require fire protection, and therefore have economic advantages.

The fire safety of these structures is ensured by the following conditions: i) the design at room temperature (or "cold design"), according to the current rules, is the basic condition for the stability of the structure in the fire situation; no additional measures for fire neither a special "hot" design are required; ii) beams with composite steel concrete section including shear studs should be used; for economic reasons, it is recommended to use light weight sections (IPE, HEAA and UB); iii) large flange sections (HEA, HEB, UC) should be considered for the columns; and iv) horizontal forces must be supported by frames or bracings (protected against fire). Additionally, CTICM [1] indicates: i) use the same cross sections for all columns in the same floor; these columns must be filled with concrete between the flanges, ii) use of concrete stairs to increase the horizontal stability and to be used as emergency stairs; iii) use a minimum steel grade of S355, and minimum concrete class of C30/37; iv) steel beams connected to the concrete slab by shear studs with a minimum degree of connection of 80%; v) concrete slabs built in situ or precast concrete; the essential point is the static and structural integration of the slab in the load-bearing system [20].

Table 1:Resistance requirements of car parking, according to INERIS [18], ECCS. [20]

| country | limitations | | | | | | General requirement for fire ISO 834 | Alternative design conditions | |
|---|---|---|---|---|---|---|---|---|---|
| | Minimum percentage of opening (%) | | Maximum | | | | | | |
| | Openings /floor | Openings /walls and facades (*1) | Dist. between opposites facades (m) | n° of stories | Building height (m) | Floor area per story ($m^2$) | | No fire protection | Natural fire (*3) |
| Germany | - | 33 | 70 | - | 22 | - | R0 (*5) | / | / |
| Austria | - | 33 | 70 | - | 22 | - | Up to R90 | Yes | Yes |
| Belgium [21] | - | 17 | 60 | - | - | - | R0 (*5) | / | yes |
| Denmark | 5 | - | 24 | - | - | - | R0 (*5) to R60 | Yes | Yes |
| Spain | - | - | - | - | - | - | R60 to R120 (*2) | - | - |
| Finland | 10 | 30 | - | 8 | - | 9000 | R60 | No (*4) | Yes |
| France [22] | 5 | - | 75 | - | - | - | Up to R60 | No (*4) | Yes |
| Netherlands | - | 30 | 54 | - | 20 | - | R0 (*5) to R30 | / | / |
| Hungary | - | - | - | - | - | - | R30 (*2) to R90 | No | No |
| Italy [23],[24] | 15 | 60 | - | - | - | - | R0 | - | - |
| Luxemburg [25] | - | 50 | - | - | - | - | R0 (*5) to R30 | / | / |
| Norway | - | - | - | - | 16 | 5400 | R10 to R60 | Yes | - |
| Poland | - | - | - | - | 25 | 4000 | R60 | No | - |
| Portugal [26] [27]. | | | | | | | R60 to R180 | - | Yes |
| U. K | 5 | - | 90 | - | 15.2 | - | R15 | Yes | Yes |
| Sweden | - | - | - | - | - | - | Up to R90 (*4) | Yes | Yes |
| Switzerland | - | 25 | 70 | - | - | - | R0 (*5) | / | / |

(*1): Total area of openings / total area of walls and facades surrounding one parking level.
(*2): General requirements of National Building Code.
(*3): Use of Natural Fire as an alternative to ISO fire to prove the fire resistance.
(*4): Bare steel is allowed if this can be proved by tests or scientific studies.
(*5): If specific structural conditions defined in National code are met.

## 2.3- Statistics of Fires in Open Car Parks

### 2.3.1- Open Car Park

Design method presented in [5] applies, as indicated from the very beginning, to the open steel car parks. According to the Building Regulations the car park is considered open if it the total area of openings (at each level) is grater then 35% of the overall wall area, and the distance between walls with openings is smaller than 100 m. These two conditions ensure the natural ventilation as it is shown in Figure 10, which helps to avoid accumulation of smoke and additional increase of temperature.

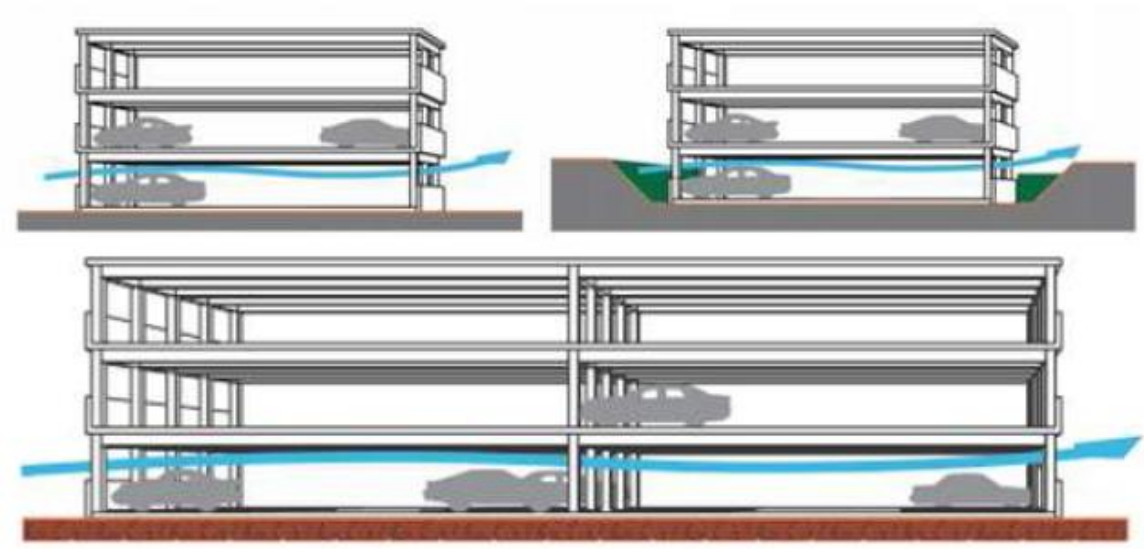

Figure 10: Natural ventilation in open car park. [5]

Some statistics of fires occurred in car parks have been realized, in order to define the car park structure and the scenario we will use for testing in Open car parks, [28]. The existing statistics in literature concerning fires in car parks are poor. The technical note n° 75 from ECSC and the final report ECCS research on Closed Car Parks of the gives a general view of the statistics of the 80's, mainly from United States. Therefore, it was necessary to get new statistics of fires in car parks.

The information about fires comes mainly from fire brigades, and particularly from the Fire Brigade of Paris (BSPP) which usually writes a report for each intervention. The statistic study is based on: 327 intervention reports from BSPP in 1997 concerning fires in underground car parks, 78 intervention reports from BSPP, concerning fires in upper-structure car parks during three years: 1995 (18 reports), 1996 (26 reports) and 1997 (34 reports).

The underground car parks are generally closed car parks and upper-structure parks are usually open car parks. Even if some upper-structure car parks are closed, the statistics will be considered representative of open car parks. Some statistics from the towns of Marseille, Toulouse, Brussels and Berlin were also included.

The intervention reports usually give the following information: - date, call time, Intervention duration, injured people, type of building, ignition of fire, propagation of fire, time to extinction, description of fire and damage.

The time to extinction is usually classified by period: 1 and 5 minutes, 6 and 15 minutes, 16 and 30 minutes, 31 and 59 minutes, 60 and 89 minutes, 90 and 119 minutes, 120 and179 minutes, 180 and 239 minutes.

The propagation is generally never described and known, and the ignition source is usually unknown. Only two or three cases are recognised. The description concerns the combustible, the problems for extinction, and description of the injured people.

The “damage” part gives the number of burning cars and some information about them: electrical problems, smoke propagation. The statistics resulting from the analysis of these reports are given in terms of time to extinction, number of cars involved in the fire, classifications of cars, injuries, daytime of fire occurrence.

The classification of cars is based on the calorific potential of cars and is given by the following Table 2.

Table 2: Classification of cars. [29]

| Manufacturer | Category 1 | Category 2 | Category 3 | Category 4 | Category 5 |
|---|---|---|---|---|---|
| Peugeot | 106 | 306 | 406 | 605 | 806 |
| Renault | Twingo-clio | Mégane | Laguna | Safrane | Espace |
| Citroen | Saxo | ZX | Xantia | XM | Evasion |
| Ford | Fiesta | Escort | Mondeo | Scorpio | Galaxy |
| Opel | Corsa | Astra | Vectra | Omega | Frontera |
| Fiat | Punto | Bravo | Tempra | Croma | Ulysse |
| Wolkswagen | Polo | Golf | Passat | // | Sharan |
| Theoretical energy | 6000 MJ | 7500 MJ | 9500 MJ | 12000 MJ | |

This type of classification is also used to classify registration numbers in France. The percentage of cars according to these 5 categories in 1995, 1996, 1997 and 1998 is given in Figure 11.

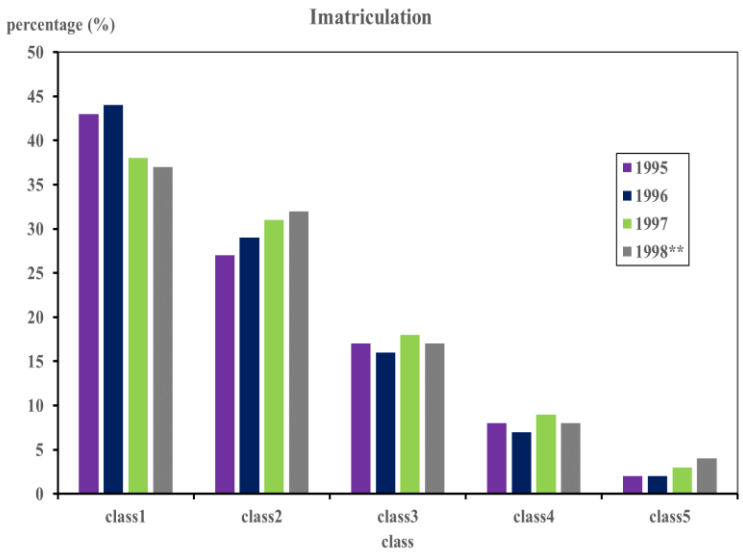


Figure 11: Distribution of car classification from the market. [29]

One can notice that a car of the 80's which is classified in category 3 according to its size represents a lower calorific potential than a car of the 90's in the same category.

The cars will be, in the present statistics, classified according to their size and not according to the potential. This assumption allows a longer use of these statistics that means, up to the time when the cars of the 80's will disappear and the cars of the 90's will represent a minority among the cars.

The previous studies of CTICM show that for example a Renault 18 classified in category 2 has a potential energy of 5700 MJ and a small car as Renault 5 of category 1 has a potential energy of 3700 MJ, lower values than the classification of the table given above.

The theoretical energy must be multiplied by a coefficient varying between 0.5 and 0.8 in order to give the energy released during the fire. The tests performed by CTICM showed that a Renault 18 released an energy of 3800 MJ (coefficient of 0.66) and a Renault 5 an energy of 2100 MJ (coefficient of 0.56). Nevertheless, it was shown that a coefficient 0.7 to 0.8 could be deduced for new cars.

## 2.4- Open Car Parks

The number of vehicles involved in the fire development in open car parks varies between 0 and 3. The number of car fires in this statistics is 55, involving a total number of 72 cars. [29]

### 2.4.1- Number of Cars Involved in a Fire

The following figure gives the percentage of cars simultaneously involved in fire. The maximum number of cars involved in fires was 3. This number corresponds to only 10 % of the fires.

We can notice that 30 % of fires are not due to cars. The combustible was: papers, garbage, materials in a box.

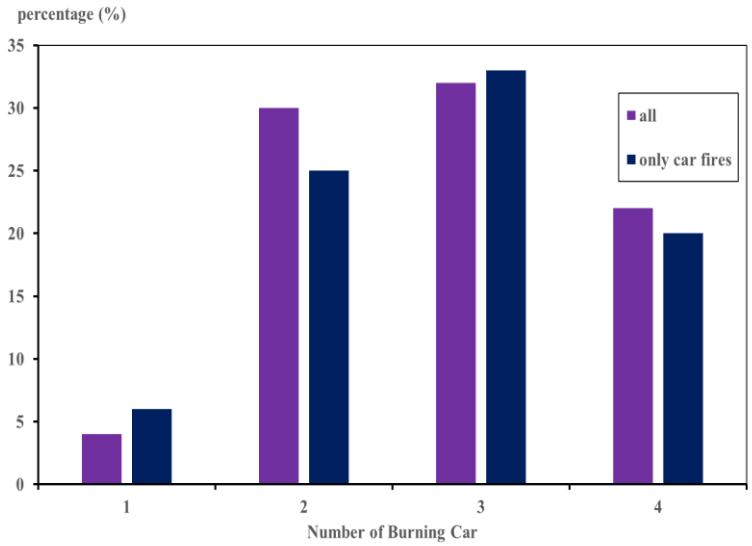


Figure 12: Number of vehicles involved in fires. [29]

### 2.4.2- Car Classification

The cars are classified according to the Table 2. Not all reports give information about the type of each car, so only 70 % of cars (50 cars) have been used to determine the distribution in category [29]. The distribution is given in the following figure. The categories 4 and 5 represent 10 % of cars.

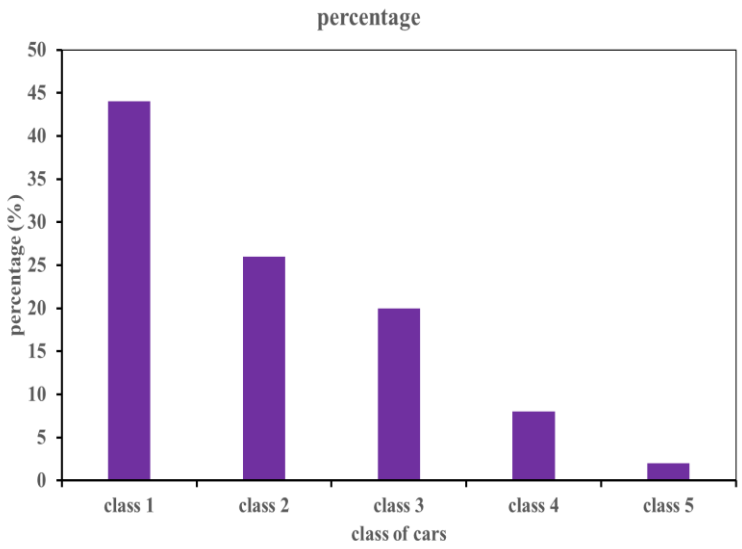


Figure 13: Classification of burning cars. [29]

### 2.4.3- Time to Extinction

Figure 14 gives the distribution of fire according to the time to extinction by the fire brigade, or before their arrival. Two kinds of distribution are used: considering all fires or considering only car fires. [29]

For car fires, 5.5 % were extinguished before the arrival of fire brigade. All fires were stopped in 1 hour. Only 9 car fires (16 % of cases) required duration between 30 minutes and 1 hour to extinguish the fire.

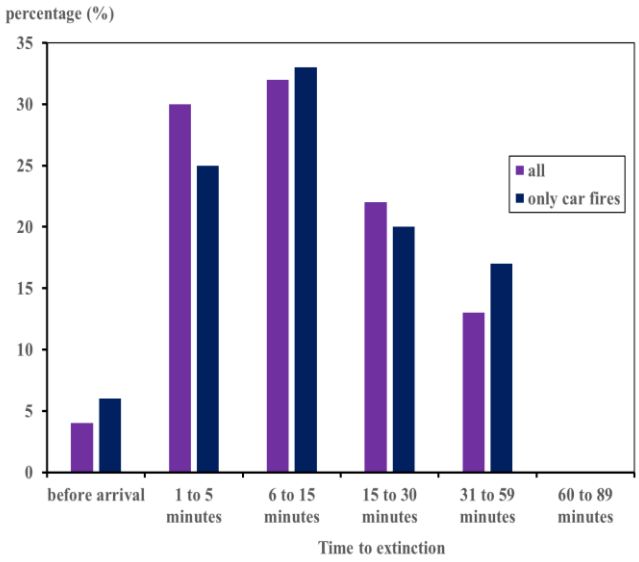


Figure 14: Time for fire extinction. [29]

# CHAPTER 3: FIRE EVENTS

## 3.1- A Heat Release Rate Models

### 3.1.1- Heat of Release Rate From Vehicles

The model of a car under fire presented in the ECCS report [2] is based on experimental fire tests: it was observed that the flames extend out of the car, mainly through the windscreen and the rear window.

The hot gases in the flames and above them move upward due to buoyancy; this flow of gases corresponds to the fire plume. The burning car is divided into two plumes, which are called as the front and the rear fire plumes (Figure 15), and the sum of the heat releases included in the two fire plumes is equal to the heat release of the vehicle.

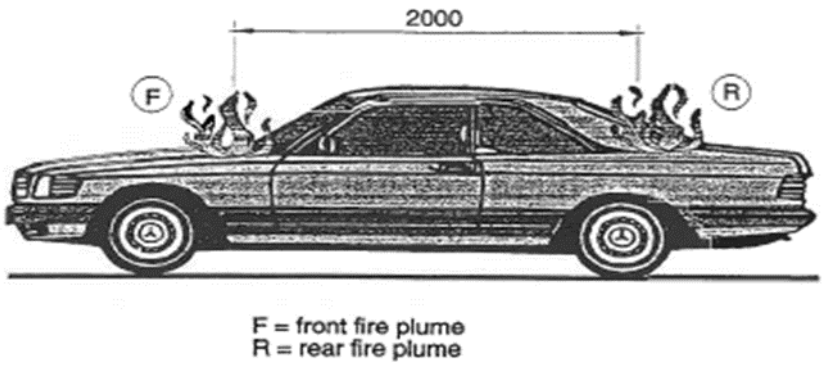


Figure 15: Front (F) and rear (R) fire plumes. [2]

In order to calculate the heat release rate, cars under fire have been experimentally studied in several countries [30]. Most of the tests were performed in closed conditions. The first tests carried out in opened conditions were developed by [31] in the 90's. The total heat release rate of a European car from the 70's burning in an open car park building is equal to 4000 MJ.

#### 3.1.1.1- Dimensions of The Parking Bay and The Car

Despite the variety in the shapes of cars it is possible, through statistical evaluations, to define the size of a «standard vehicle and of a standard parking bay (5.0m long and 2.5m

wide). The fire model defined can be applied to any car of the parking. A car situated in a parking bay with both fire plumes is shown on Figure 16.

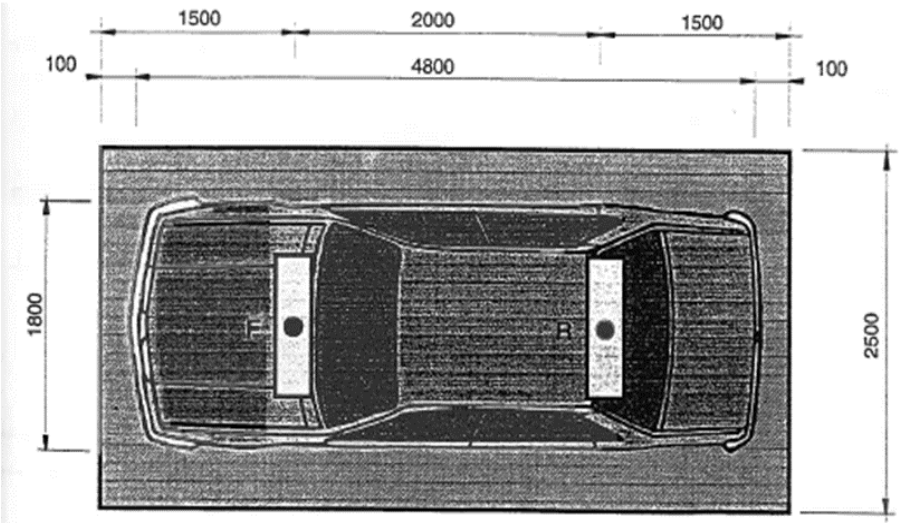


Figure 16: The parking bay. [2]

Between 1993 and 1996, the European project *-Development of design rules for steel structures subjected to natural fires in closed car parks* [32] developed a design guide for closed car park structures subject to localised Natural Fires and established more realistic standards in Europe. Within this project, 10 full-scale calorimetric fire experiments on old and recent European cars were performed by CTICM. In the first six tests, class 3-cars from the 70's and 80's were tested, while in the last four tests, newer cars (reference time: 1995) were used to simulate an open car park.

Based on these tests, reference curves of the rate of heat release for two class 3-cars (one car as fire source and another one subject to the spread of fire with 12 minutes of delay) were defined. These curves allow simulating multiple burning cars 3 presents the references curves for three consecutive burning class 3-cars, with maximum 8.3 MW. For commercial vehicles, CTICM suggests a maximum value of rate of heat release equal to 18 MW, this value is considered as a "safe value" for design, but this is not a measured value. [2]

### 3.1.2- The HRR Model

When considering the Heat Release Rate curve in Figure 17 it was noted that certain peaks can be seen above the evident overall burning of the car. These peaks can be regarded as results of the burning of certain fire load concentrations [2]. They are located along the time

axis according to the stages of the fire spread in the car. The HRR model function is composed of an overall burning component and components representing the peak values. For the former one Boltzmann curve according to Eq (3- 1) is chosen and for the RHR peaks three Gaussian curves of Eq (3-2) were selected.

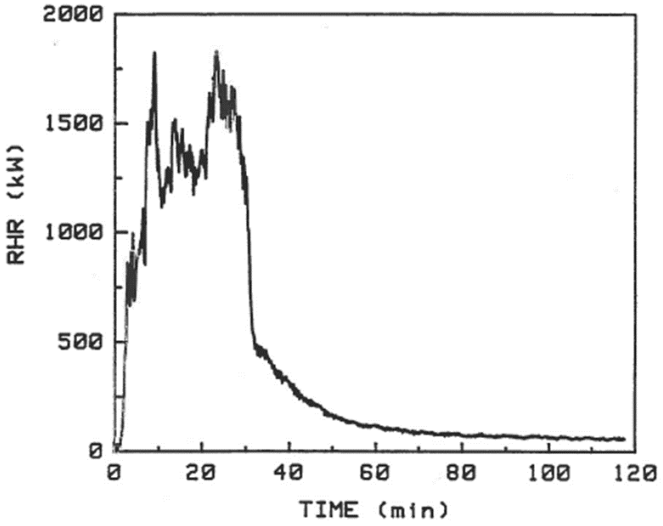

Figure 17: The heat release rate in function of time. [2]

$$Q_1(t) = Q_{10}(t - t_1)^{1/2} \exp(-(t - t_1)/a_1) \quad \text{Eq. (3-1)}$$

$$Q_i(t) = Q_{i0} \exp(-(t - t_i)/a_i)^2) \cdots; i = 2...4 \quad \text{Eq. (3-2)}$$

These components include three parameters in form of coefficients $Q_{i0}$, $a_i$ and $t_i$, which allow them to be modified for fitting. $Q_{i0}$ defines the magnitude of the HRR, $a_i$ , the shape of the curve and $t_i$ , the time shift.

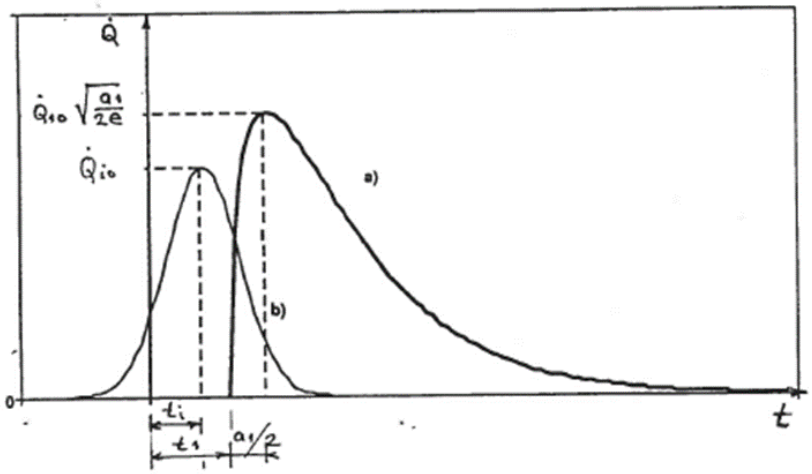

Figure 18: HRR model functions: a) Boltzmann function, b) Gaussian function. [2]

The heat release rate from the whole car Q(t) is then given as the sum of the components by

$$Q_{car} = Q_1(t) + Q_2(t) + Q_3(t) + Q_4(t) \qquad \text{Eq. (3-3)}$$

The HRR curve from the whole car, Eq (3-3), was fitted to the measured HRR curve by inspection and the total energy released according to the fitted HRR curve was fixed to the measured total energy released. The parameters used in the curve fitting are presented in Table 3.

Table 3: Parameters used in the curve fitting. [2]

| **Test** n° | $\mathbf{Q_{10}}$ ($kWs^{-1/2}$) | $\mathbf{Q_{20}}$ ($kWs^{-1/2}$) | $\mathbf{Q_{30}}$ ($kWs^{-1/2}$) | $\mathbf{Q_{40}}$ ($kWs^{-1/2}$) | $\mathbf{a_1}$ (s) | $\mathbf{a_2}$ (s) | $\mathbf{a_3}$ (s) | $\mathbf{a_4}$ (s) | $\mathbf{t_1}$ (s) | $\mathbf{t_2}$ (s) | $\mathbf{t_3}$ (s) | $\mathbf{t_4}$ (s) |
|---|---|---|---|---|---|---|---|---|---|---|---|---|
| 1 | 25.8 | 1000 | 0 | 1000 | 1700 | 500 | 0 | 500 | 180 | 900 | - | 2220 |
| 2 | 10.3 | 1500 | 1100 | 1500 | 2400 | 216 | 216 | 396 | 180 | 600 | 1020 | 1620 |
| 3 | 25.8 | 1100 | 1300 | 700 | 2222 | 256 | 256 | 507 | 180 | 510 | 870 | 2280 |
| Mean | 20.6 | 1200 | 800 | 1067 | 2107 | 324 | 157 | 468 | 180 | 670 | 945 | 2040 |

The mean values of coefficients $Q_{i0}$ , $a_i$ and $t_i$, of the components are calculated. They have been written in the bottom row of Table 3 When this average HRR curve is then normalized with respect to the total energy release of 4 GJ by increasing the coefficient $Q_{i0}$ we come to the parameter values of Table 4.

Table 4: The average HRR curve normalized to 4.0 GJ total energy release. [2]

| $\mathbf{Q_{10}}$ ($kWs^{-1/2}$) | $\mathbf{Q_{20}}$ ($kWs^{-1/2}$) | $\mathbf{Q_{30}}$ ($kWs^{-1/2}$) | $\mathbf{Q_{40}}$ ($kWs^{-1/2}$) | $\mathbf{a_1}$ (s) | $\mathbf{a_2}$ (s) | $\mathbf{a_3}$ (s) | $\mathbf{a_4}$ (s) | $\mathbf{t_1}$ (s) | $\mathbf{t_2}$ (s) | $\mathbf{t_3}$ (s) | $\mathbf{t_4}$ (s) |
|---|---|---|---|---|---|---|---|---|---|---|---|
| 24 | 1400 | 930 | 1240 | 2110 | 330 | 160 | 470 | 180 | 670 | 945 | 2040 |

The total normalized average HRR curve. $Q_{car}$ and its components Qi(t) are shown in Figure 19

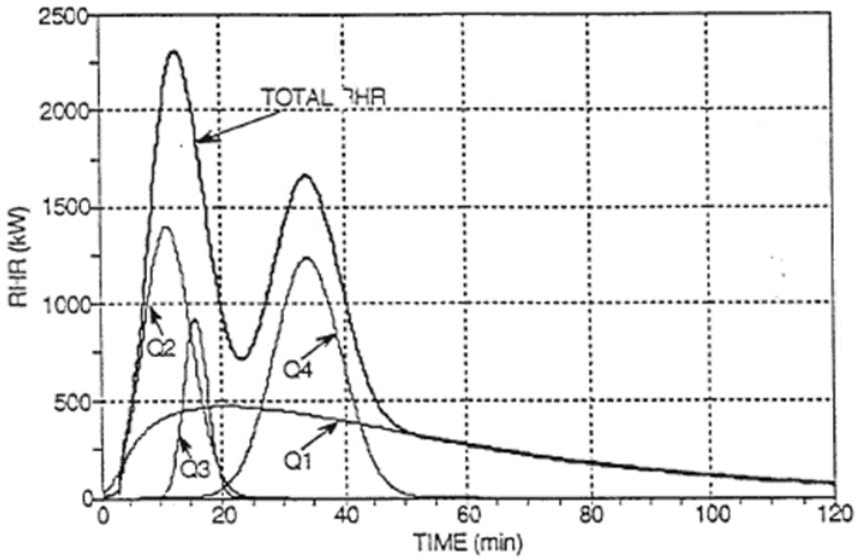


Figure 19: Total average HRR curve and its components. [2]

The energy contents of the components of the total normalized HRR function can be calculated by integration over the Qi-curves with respect to time. The results are given in Table 5.

Table 5: Energy content in the average HRR curve normalized to 4.0 G J. [02].

| $\int Q_1 dt$ | | $\int Q_2 dt$ | | $\int Q_3 dt$ | | $\int Q_4 dt$ | | $\int Q_{front} dt$ | | $\int Q_{rear} dt$ | | $\int Q_{car} dt$ |
|---|---|---|---|---|---|---|---|---|---|---|---|---|
| (GJ) | (%) | (GJ) | (%) | (GJ) | (%) | (GJ) | (%) | (GJ) | (%) | (GJ)…..(%) | | (GJ) |
| 1.89 | 47 | 0.82 | 20 | 0.26 | 7 | 1.03 | 26 | 1.76 | 44 | 2.24 | 56 | 4.0 |

### 3.1.2.1- HRR Model For Rear and Front of Vehicles

During the fire tests described in [02] it was clearly observed that flames extended out of the car mainly through the windscreen and the rear window. The hot gases in the flames and above them move upwards due to the buoyancy. This buoyant flow is referred to as a fire plume.

The burning car is divided into two plumes which are called as the front fire plume and the rear fire plume.

The axes of the fire plumes are assumed to be 2 m apart according to the dimensions of ordinary passenger cars. This is shown in Figure 20. For distance H the fire level in a car fire can be approximated to 0.3 m above the floor level. The sum of the rates of heat release included in these plumes equals to the total heat release of Eq (3-3) and the parameters of Eqs (3-1) and (3-2)

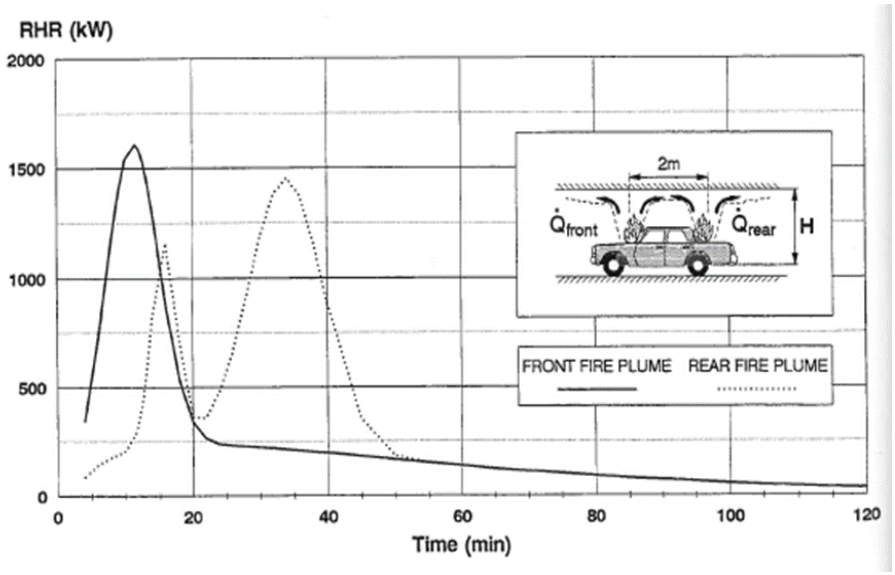


Figure 20: Front and rear tire plumes of the car tire model. [2]

The four parts of the total heat release in Eq (3-3) are divided into the front and rear fire plumes as follows:

$$Q_{front}(t) = 0.5Q_1(t) + Q_2(t) \qquad \text{Eq. (3-4)}$$

$$Q_{rear}(t) = 0.5Q_1(t) + Q_3(t) + Q_4(t) \qquad \text{Eq. (3-5)}$$

The parts $Q_{1,}$ ..., $Q_4$ of HRR can be interpreted to correspond to the following fire load concentrations: $Q_1(t)$ the passenger cabin, $Q_2(t)$ the engine and the front tyres, $Q_3(t)$ the boot and the rear tyres, $Q_4(t)$ the fuel. The magnitude of each part can be seen in Table 5.

### 3.1.2.2- HRR New model of Cars

A car fire campaign was realized in 1995 at the CTICM laboratory. Ten car fire tests were performed involving eighteen cars. Four tests were relevant to cars manufactured in 1994-95. Within the European research "Demonstration test is car parks and large volume", three car fire tests were performed in a real car park made of unprotected steel structure. In order to have information about the fire characteristics of cars used in the demonstration tests, two new tests have been performed under calorimeter hood at the CTICM laboratory. The present report gives information about Peugeot 406 break fire and Peugeot 406 family fire.

It has been already mentioned that to specify fire scenario it is necessary to know rate of heat release (HRR) of the cars. HRR is a measure of Megawatts produced by a burning item in time [MW]. This value is determined experimentally by setting a car on fire under calorimetric hood as shown in next figure.

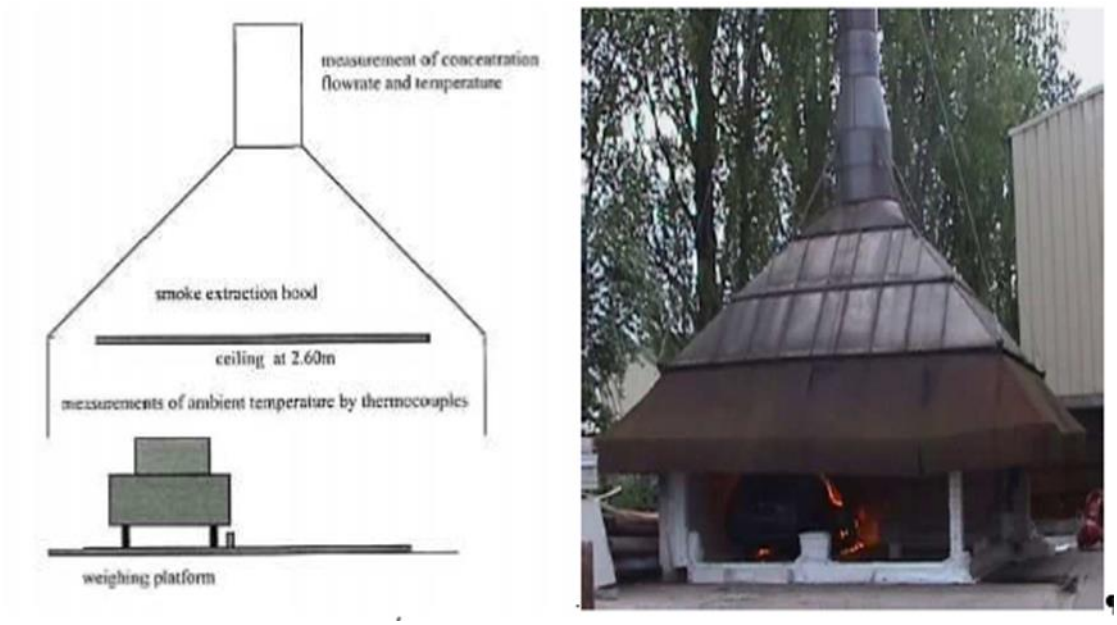


Figure 21: The calorimetric hood. [3]

In general, during the tests, the cars were equipped as in practice with oil, 4 tyres and a spare tire, and the fuel tank was 2/3 full.

10 tests were carried out in 1995 and 1996, involving 15 cars of old (70ies/80ies) and new generation (90ies): 5 tests were performed with one car and the 5 others with 2 cars.

In the first 7 tests, the car was ignited with 1.5 l of the petrol in an open tray under the left front seat. The left front window was completely open, and the right front window was half open. All doors were closed. In the case of test with two cars, the doors and windows of the second one were closed.

In the last 3 tests, the cars were ignited under the car at the gear box level with 1 litre of petrol, as a testing procedure sometimes used by car manufactures.

Results in terms of rate of heat released using oxygen consumption technique, on a car of the 3rd category (of old and new generation) are shown on Figure 22.

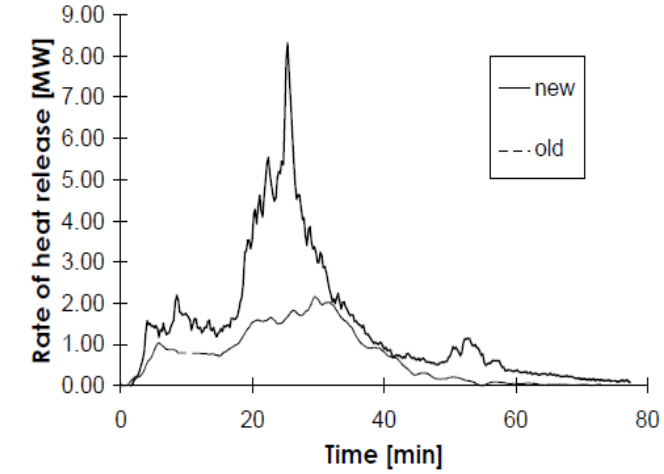


Figure 22: Old and new Heat Release Rate. [29]

Vehicles tested under calorimetric hood were equipped as if they were in operating state. They had four tires and one spare wheel, a tank filled in two thirds of its capacity with petrol. Additionally, the cars had airbags and air conditioning. All the doors and windows were closed when the car is set on fire with 1.5 litters of petrol. The car was equipped with thermocouples.

According to [10] the heat release rate depends on time for each categories of vehicle and are shown in the table below and represented in Figure 23.

Table 6: The HRR of different car categories.

| | Vehicles categories | | | | |
|---|---|---|---|---|---|
| | Category 1 | Category 2 | Category 3 | Category 4 | Category 5 |
| Time | HRR | HRR | HRR | HRR | HRR |
| min | kW | kW | kW | kW | kW |
| 0 | 0 | 0 | 0 | 0 | 0 |
| 4 | 884 | 1105 | 1400 | 1768 | 1768 |
| 16 | 884 | 1105 | 1400 | 1768 | 1768 |
| 24 | 3474 | 4342 | 5500 | 6947 | 6947 |
| 25 | 5242 | 6553 | 8300 | 10448 | 10448 |
| 27 | 2842 | 3553 | 4500 | 5684 | 5684 |
| 38 | 632 | 789 | 1000 | 1263 | 1263 |
| 70 | 0 | 0 | 0 | 0 | 0 |

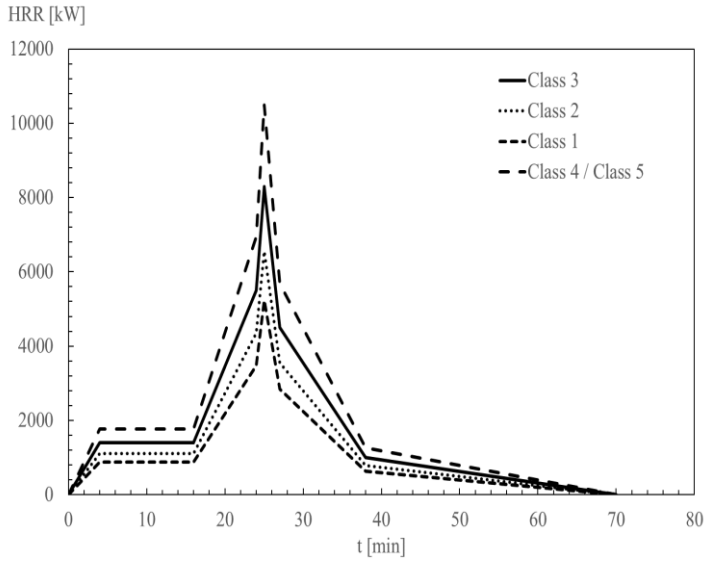


Figure 23: Curves of rates of heat release for the 5 classes of cars.

From the table above, during 70 minutes of tests, it seems that the maximum heat release rate of burning cars are 5242 kW for the first class and 6535 kW for the second, 8300 kW for the third class and 10448 kW for both cars of class fourth and fifth. The maximum energy released is always expected at 25 min after fire ignition.

According to the tests developed in 1995 and 1996 car class 3 was considered, being the heat release rate for burning 3 cars of class 3 given here below.

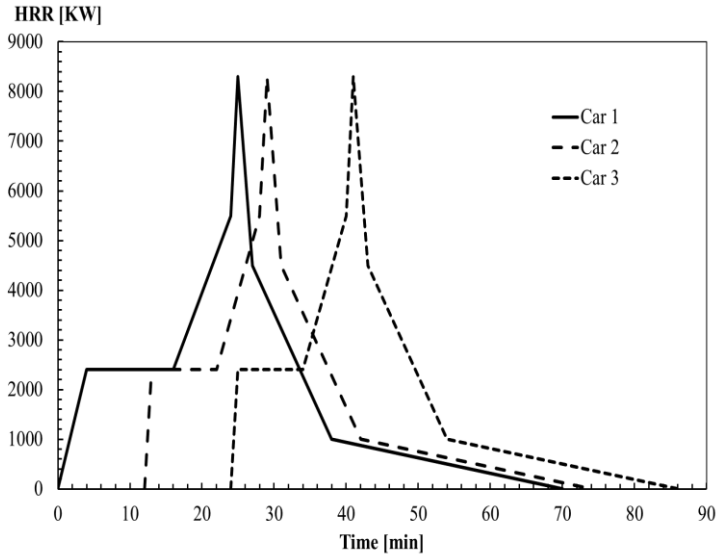


Figure 24: Reference curves HRR vs time of the three burning class 3-cars [29].

Table 7: The HRR for 3 burning cars [29].

| Time (min) | Car 1 [MW] | Time (min) | Car 2 [MW] | Time (min) | Car 3 [MW] |
|---|---|---|---|---|---|
| 0 | 0 | 12 | 0 | 24 | 0 |
| 4 | 1.4 | 13 | 2.4 | 25 | 2.4 |
| 16 | 1.4 | 22 | 2.4 | 34 | 2.4 |
| 24 | 5.5 | 28 | 5.5 | 40 | 5.5 |
| 25 | 8.3 | 29 | 8.3 | 41 | 8.3 |
| 27 | 4.5 | 31 | 4.5 | 43 | 4.5 |
| 38 | 1 | 42 | 1 | 54 | 1 |
| 70 | 0 | 74 | 0 | 86 | 0 |

The HRR curve of a utilitarian vehicle is given in Figure 25 in blue colour, with two more curves of a burning class 3-car at the beginning (in red) and a burning class 3-car after propagation (in blue). The maximum HRR value of the utilitarian vehicle (18MW) is not obtained by experimental work but corresponds to a safe value [1].

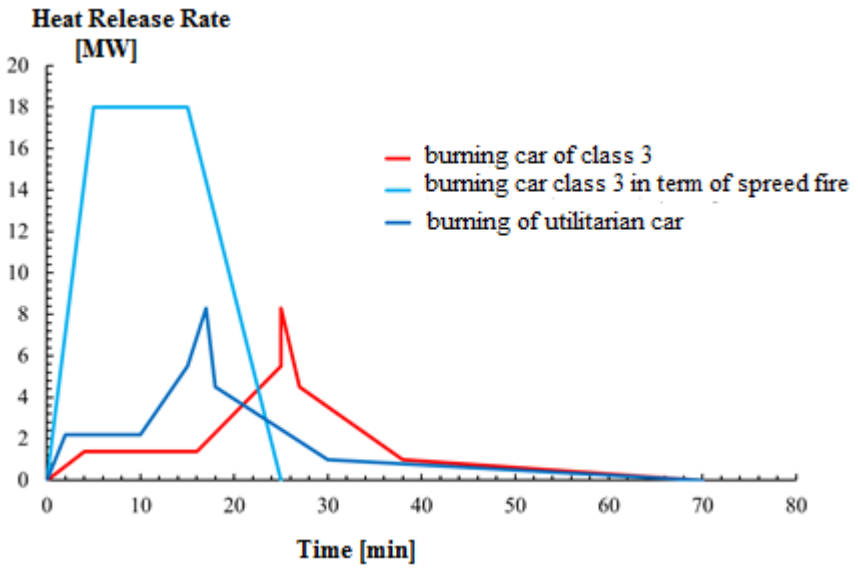


Figure 25 : Reference curves HRR of a burning utilitarian vehicles and class 3 cars. [1]

Figure 26 shows HRR curves obtained for the fire scenarios number 5, including 7 vehicles [15] and represented in dark blue in the figure, and fire scenario number 6, including 4 vehicles and represented in blue grey in the figure, with a utility vehicle in the second position of burning. The fire scenario number 3, with only a utility vehicle burning under a beam.

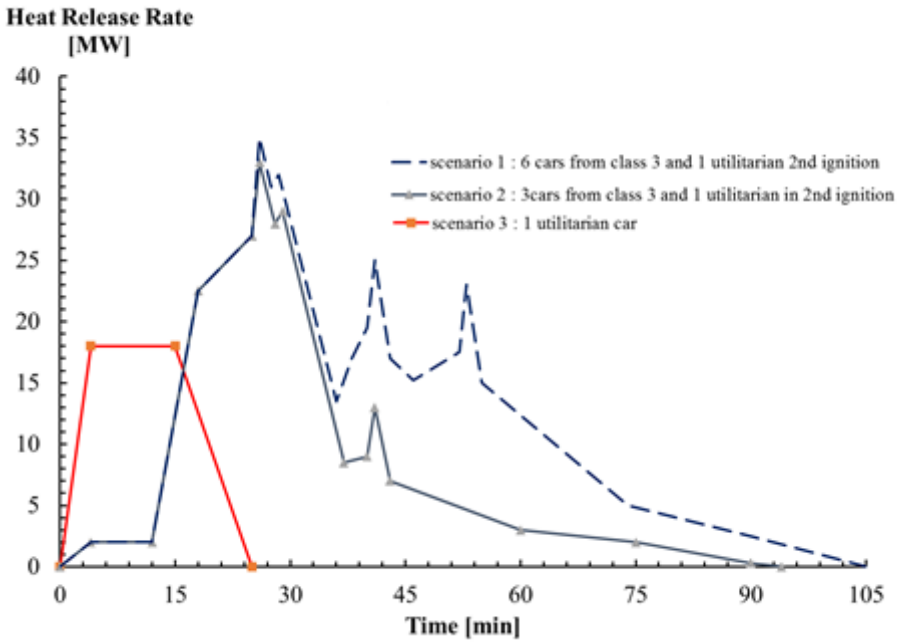


Figure 26: Reference curves HRR (MW) vs time (min) according to the scenario. [1]

### 3.2- Fire Scenarios

In order to define some fire scenarios, this car park structure was chosen (see Figure 30). In this work, one fire scenario was identified to be representative of their effect of the steel structure. The fire event of a class 3 vehicle was considered to define all these possible scenarios: Fire scenario 1 with one car burning below the secondary beam (IPEA 600) at mid-span (most severe case); Fire scenario 2 with two cars burning below the main beam (HEAA650) and; Fire scenario 3 with three cars burning near the columns (HEM 300).

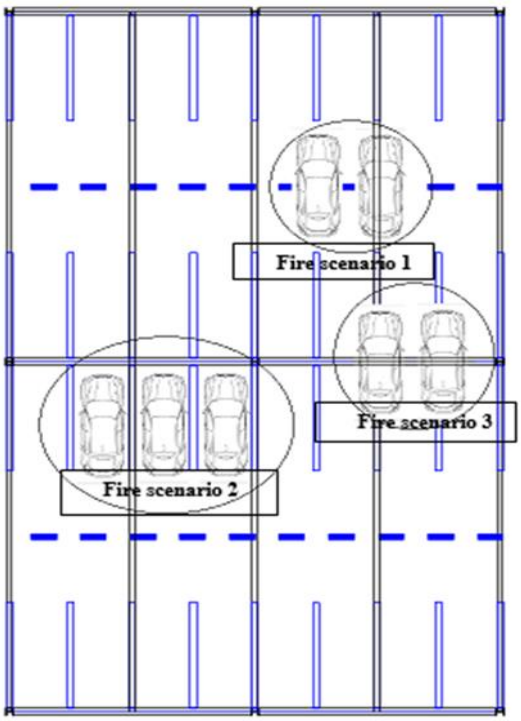


Figure 27: Most important fire scenarios.

The fire scenario 1 will be choose to this study, one car burning in the mid span of the secondary beam IPEA600. Different fire events categories of cars (classes) will be consider to analysed the effect of the localised fire at the resistance of the unprotected steel beam of the open car park.

The position of the vehicles should represent the most unfavourable situation for the elements (or substructure). The vehicles' type mostly used in fire scenarios are classified according their calorific potential or combustion energy. Five car classes of cars were already defined [8], being the energy for class 1 - equal to 6000 MJ (ex. Peugeot 106), the energy for class 2 equal to 7500 MJ (ex. Peugeot 306), the energy for class 3 equal to 9500 MJ (ex. Peugeot 406) and the energy for classes 4 and 5 equal to 12 000 MJ (ex. Peugeot 605).

According to statistical studies of actual fires in car parks, 90% of the vehicles involved in a fire are classified as class 1, 2 or 3. The INERIS " Institute National de environment Industrial et des Risques" considers that fire scenarios with cars of class 3 should be used to evaluate the structural stability of the car park under fire, and the fire resistance of the structure should be ensured during the entire fire scenario, or at least, if allowed by National requirements, up to a certain resistance time R of the elements defined by the standard ISO curve. In addition, a scenario including a commercial vehicle corresponds to an extreme

situation and should only be used to check the global behaviour of the structure, assuming local collapse, without progressive collapse [1].

The first fire scenario implies only one car burning at mid-span under the secondary beam R=0 m. It corresponds to the maximum bending moment position and so the most critical situation for the beams. Only one burning car has been supposed because it is not realistic to have simultaneously two cars which are property parked, burning, and just beneath the steel beam and at mid-span. The height between the source of heat and the bottom flange of the beam is assumed to be $H_s$= 2,1 m, and the other parameter are identified in next chapter.

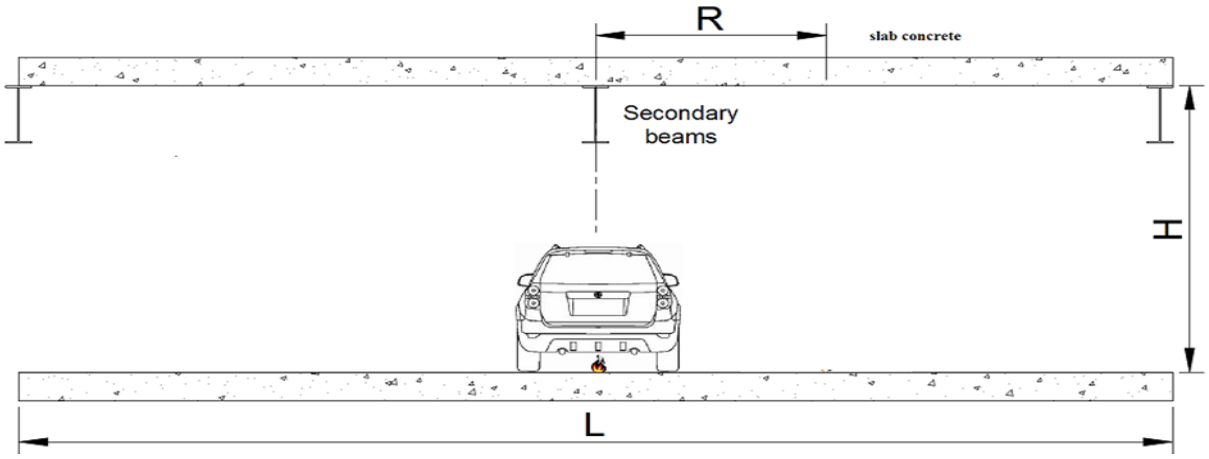


Figure 28: The lateral view of fire scenario 1.

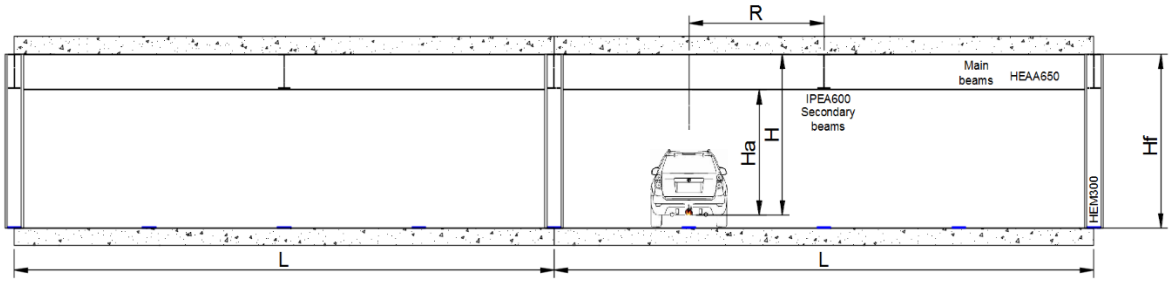


Figure 29: The front view of the fire scenario 1.

### 3.3- Dimensions of The Structure

The chosen structure (see figure 27) is composed of three rows of three columns joined by ten secondary beams of 16 m and six main beams of 10 m. The cross section of the columns is a HEM 300. The cross section of the secondary beam is IPE A 600, and the cross section of the main beam is HEAA 650 connected to a 22cm with concrete slab. The distance between the secondary beams is 5.0m and the distance between the main beam is 16 m.

The structure was designed according to Eurocodes and optimized in order to be just sufficient to bear the loads with the safety required.

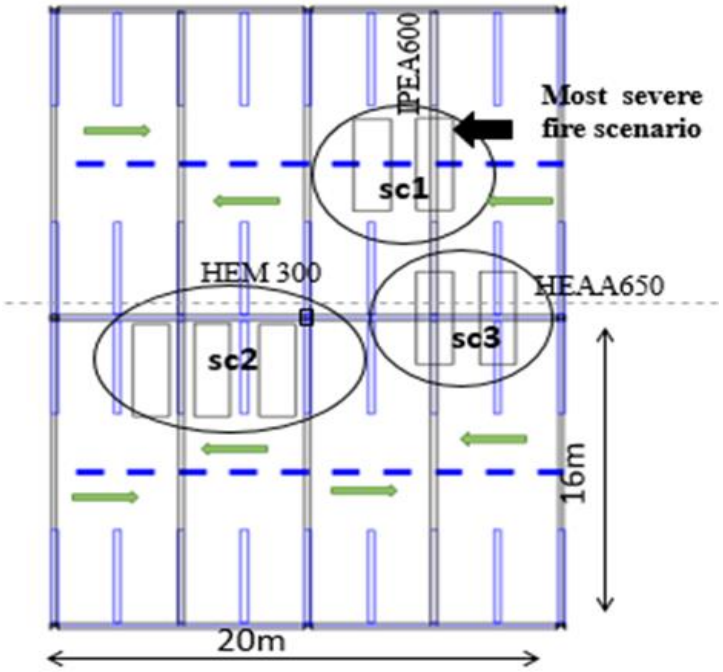


Figure 30: Top view of the car park used for study.

## CHAPTER 4: METHOD OF ANALYSIS

### 4.1- Localized Fire

Fire starts as a small localized fire and cease to be only when flashover occurs. Even a localized fire can have a significant effect on the structure, depending on the building type and the relative position of the fire to the structural elements.

The thermal effect on horizontal elements located above the fire also depends on their distance from the fire. It can be assessed by specific models for the evaluation of the local effect on adjacent elements, such as Heskestad or Hasemi method. The Two models are presented in Annex C of Eurocode 1992-1-2 [3] for the effect of a localized fire.

#### 4.1.1- Heskestad Model

Thermal action of a Localised fire can be assessed by using the Heskestad method. Differences have to be made regarding the relative height of the flame to the ceiling.
The flame lengths $L_f$ of a localised fire is given by:

$$L_f = -1{,}02D + 0{,}25Q_c^{2/5}(z - z_0)^{-5/3} \qquad \text{Eq. (4-1)}$$

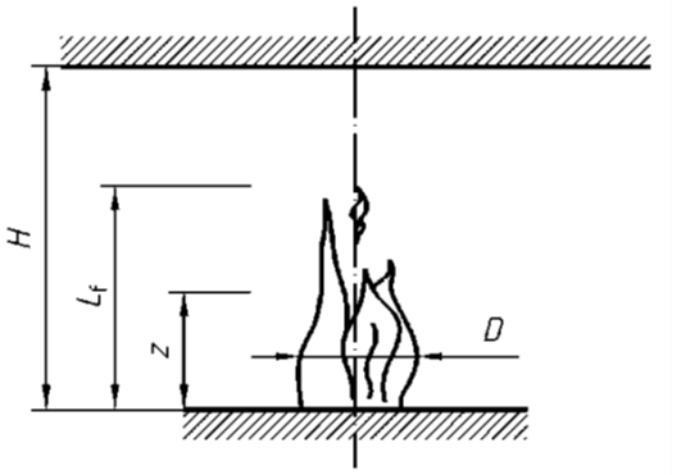


Figure 31: The Length of the flame is not touching the ceiling (Heskestad). [3]

Figure 31 shows the length $L_f$ of the flame when the fire source rests on the ground and that the flame does not touch the ceiling ( $L_f < H$ **)**, where D is the diameter of fire source.

The temperature $\theta_{(z)}$ in the plume along the symmetrical vertical flame axis is given by:

$$\theta_{(z)} = 20 + 0{,}25 Q_c^{\,2/5} (z - z_0)^{-5/3} \qquad \text{Eq. (4-2)}$$

Where: $D$ is the diameter of the fire [m], see Figure 31, $Q$ is the Heat Release Rate [W] of the fire, $Q_c$ is the convective part of the rate of heat release [W], with $Q_c = 0{,}8\,Q$ by default, $Z$ is the height [m] along the flame axis, see Figure 31, $H$ is the distance [m] between the fire source and the ceiling, see Figure 31, and $Z_0$ the virtual origin of the axis is given by:

$$Z_0 = 0{,}00524 Q^{0{,}4} - 1{,}02 D \qquad \text{Eq. (4-3)}$$

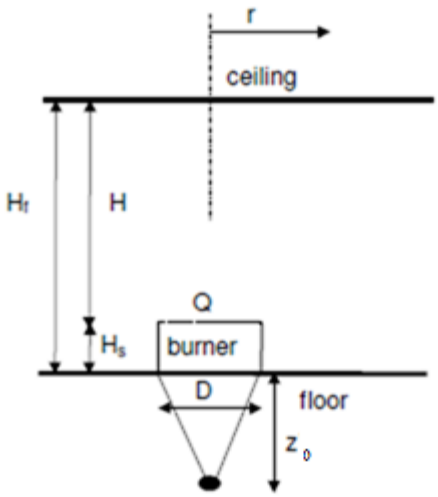


Figure 32: The Virtual Origin of flame.

### 4.1.2- Hasemi Model

The Hasemi method is a simple tool for assessing the effects of a localized fire on horizontal structural elements located above the fire. When the $L_f$ of flame is impacting on the ceiling, a different model is used. The parameters for this model is in the Figure 33 below. when ($L_f \geq H$ **).**

The scope of this model is based on Eurocode, limited to situations where the diameter D of the fire source model is not greater than 10 meters and the heat release rate of fire emitted less than 50 MW. The method is described in the Annex C, Eurocode 1992-1-2 [3].

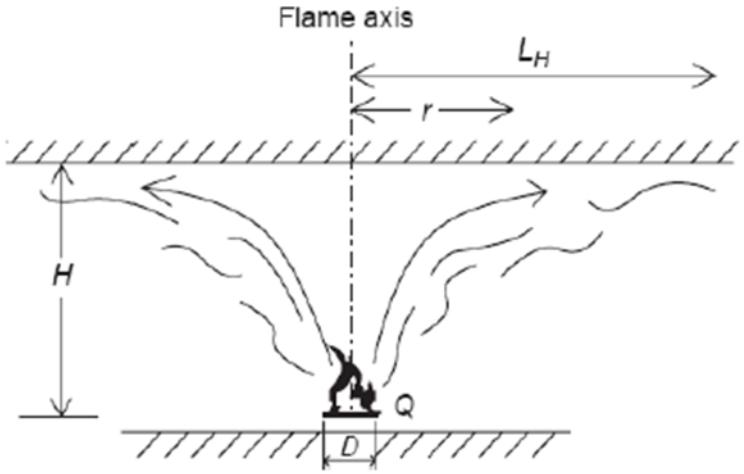


Figure 33: The Length of the flame is touching the ceiling (Hasemi). [3]

In the analysis of the open car park it is accepted hypothesis that the fire is impacting the ceiling and therefore HASEMI method of calculation is applied. When the car is burning, the fire is in fact localised fire. It means that the heat flux is determined from that car, being the heat flux to beam calculated by the following system.

The heat flux to a beam is a function of the following parameters: Rate of heat release of cars: $Q$, Height of the lower flange of the beam from the floor: $H_a$, Diameter of the fire: $D$ (2 m is used), Distance from the beam section to the car centre: $r$, Height of the fire source from the floor: $H_s$ (0.3 m is used).

The heat flux $\dot{h}$ is calculated with the Hasemi method by the following equations:

$$\begin{cases} y < 0.30 & \dot{h} = 100 \\ 0.30 < y < 1.00 & \dot{h} = 136.30 - 121.00y \\ 1.00 < y & \dot{h} = 15y^{-3.7} \end{cases} \qquad \text{Eq. (4-4)}$$

where y is the non-dimensional parameter [-] calculated by:

$$y = \frac{r + H + Z'}{L_H + H + Z'} \qquad \text{Eq. (4-5)}$$

With $L_H$ is the horizontal length of the flame [m] determined by:

$$L_H = 2.90.H.Q_H^{*\,0.33} - H \qquad \text{Eq. (4-6)}$$

And

$$H = H_a - H_s \qquad \text{Eq. (4-7)}$$

$$Q_H^* = \frac{Q}{1.11.10^6.H^{2.5}} \qquad \text{Eq. (4-8)}$$

$$Q_D^* = \frac{Q}{1.11.10^6.D^{2.5}} \qquad \text{Eq. (4-9)}$$

Where $Q_H^*$ and $Q_D^*$ are the non-dimensional heat release rates [-].

$$\begin{aligned} Q_D^* < 1.00 \quad & Z' = 2.4..D.(Q_D^{*\,2/5} - Q_D^{*\,2/3}) \\ Q_D^* \geq 1.00 \quad & Z' = 2.4.D.(1.0 - Q_D^{*\,2/5}) \end{aligned} \qquad \text{Eq. (4-10)}$$

In case of a several localised fires the heat flux received by an element of structure corresponds to the sum of heat flux obtained by each of the localised fires. However, the total heat flux is limited to max of 100 kW/m² following Annex C of EN 1992-1-2.

### 4.2- Calculation The Thermal Loading

From the thermal actions determined to the previous section towards the elements of structure, the temperatures reached by the elements of structure are determined according to time. When the field of temperature in the elements of structure is not homogeneous, the calculation of the heat transfer must be performed by means of software considering the heat transfer in “at least” 2 dimensions. When the temperature field is considered as homogeneous, the simplified model of calculation according to the Eurocode 3 Part 1-2 [4] can be used.

From the total heat flux received by the structure, the net heat flux net $\dot{h}$ received by the fire exposed per unit of surface area on the level of the ceiling needs to be calculated. The net heat flux calculation considers the heat flux from the localize effect and the heat flux loosed to the cold layer, by radiation and convection.

$$\dot{h}_{net} = \dot{h} - \alpha_c (T_s - 20) - \phi \varepsilon_m \varepsilon_f \sigma \left[ (T_s + 273)^4 - (20 + 273)^4 \right] \quad \text{Eq. (4-11)}$$

Where $\alpha_c$ represents the coefficient of heat transfers by convection, $T_s$ represents the surface temperature of the element [C °], $\Phi$ represents the shape factor, $\varepsilon_m$ accounts for the emissivity of the surface of the element, $\varepsilon_f$ represents the emissivity of the fire and finally $\sigma$ represents Stephen Boltzmann's constant ($\sigma = 5.67.10^{-8} W/m^2.k^4$).

The temperature in the upper layer can be considered as the average value of the temperature field in the gas, in fact, the thermal impact of a localised fire can be much more severe on structural elements located in the vicinity of the flames than the impact coming from the air at the average temperature. As a consequence, if the failure of the structural elements located close to a fire may be critical for the stability of the whole structure, then the average temperature is sufficient, and the localised effect of the fire must be taken into account [33].

The heat flux to the element $\dot{h}$ may be calculated by the Hasemi model, which depends on the heat released rate developed by the fire. This quantity also depends on the diameter of the fire and on the relative position of the steel element and the localized fire.

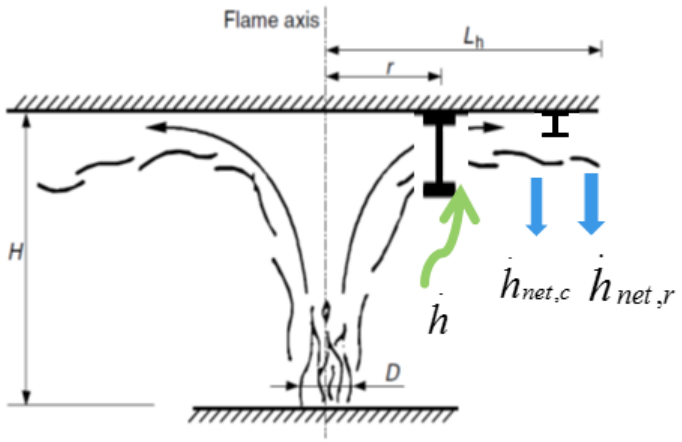


Figure 34: The heat flux received to the beams

The thermal equilibrium of the steel beam needs to consider the net heat flux at the boundaries of a steel profile $\dot{h}_{net}$. This net heat flux also considers the amount of heat flux by convection and radiation, leaving the steel beam, see Figure 34 and Eq. (4-12).

$$\dot{h}_{net} = \dot{h} - \alpha_c (T_s - 293) - \phi \varepsilon_m \varepsilon_f \sigma \left[ (T_s + 273)^4 - (20 + 273)^4 \right] \qquad \text{Eq. (4-12)}$$

The Hasemi model does not allows the calculation of the gas temperature. To overcome this difficult, a different section factor should be considering, assuring that this net heat flux is zero. This hypothesis means that the temperature of the steel profile is must equals the temperature of the surrounding gas. This temperature is defined has effective local temperature $T_{loc}$ that has the same effect on steel elements as the net heat flux calculated with this method. It is indeed the temperature of steel profile with a very high massivity. This steel profile has a temperature which is very close to the gas temperature, thus we have: $T_{loc} = T_{gas} = T_{steel}$ . $T_{gas}$ is then obtained by solving Eq. (4-13) see Figure 34.

$$\dot{h} = \alpha_c .((T_{gas} + 273) - 293) - \Phi \varepsilon_f \varepsilon_m .5.67.10^8 [(T_{gas} + 273)^4 - 293^4] \qquad \text{Eq. (4-13)}$$

The heating of unprotected or protected steel profile may be calculated with the solution methods presented in ENV1993-1-2.

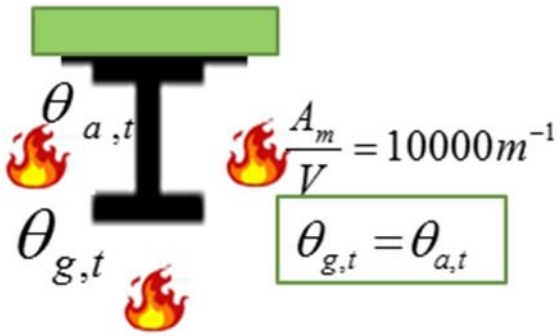


Figure 35: The temperature of steel profile with a very high section factor.

The Newton Raphson method is going to be used for solving a non-linear equation (4-15). This solution method is illustrated in Figure 36 and is going to provide the gas temperature near the steel element.

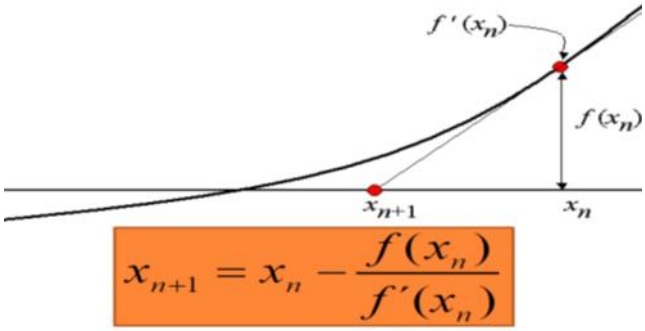


Figure 36 : Newton Raphson method.

The iterative procedure uses a trial value of gas temperature. The solution method is applied to equation (4-16) using 10 iterations to get the constant value of the new gas temperature. Usually three or four iterations are needed.

$$T_{gas}^{\,n+1} = T_{gas}^{\,n} - \frac{f(T_{gas})}{f'(T_{gas})} \qquad \text{Eq. (4-14)}$$

$$\dot{h}_{net} = 0 \qquad \text{Eq. (4-15)}$$

$$f(T_{gas}) = 0$$
$$\Leftrightarrow \dot{h} - \alpha_c.((T_{gas}+273)-293) - \Phi\varepsilon_f\varepsilon_m.5.67.10^8[(T_{gas}+273)^4 - 293^4] = 0 \qquad \text{Eq. (4-16)}$$

$$f'(T_{gas}) \Rightarrow -\alpha_c. - \Phi\varepsilon_f\varepsilon_m.5.67.10^8 \times 4 \times [(T_{gas}+273)^3] \times 1 \qquad \text{Eq. (4-17)}$$

This example took from the solver of the newton Raphson method for the calculation of the temperature of the gas for specific time (t=16 min) during the event of a car fire.

Table 8: Example of calculation with the solver of Newton Raphson

| time | 16 min | | | | |
|---|---|---|---|---|---|
| | ITER | ºC Tgas | F(X) | F'(X) | ºC Tgas new |
| | 1 | 800 | -41707 | -221 | 611 |
| | 2 | 611 | -8661 | -135 | 547 |
| | 3 | 547 | -732 | -113 | 541 |
| | 4 | 541 | -7 | -111 | 541 |
| | 5 | 541 | 0 | -110 | 541 |
| | 6 | 541 | 0 | -110 | 541 |
| | 7 | 541 | 0 | -110 | 541 |
| | 8 | 541 | 0 | -110 | 541 |
| | 9 | 541 | 0 | -110 | 541 |
| | 10 | 541 | 0 | -110 | 541 |

### 4.2.1- Thermal Properties of Steel

The calculation of the material temperature depends on the material properties. The next sections provide the information about the steel thermal properties.

#### 4.2.1.1- Specific Heat

The specific heat of the steel $C_a$ should be determined from the following in J/kgK:

$20°C \le \theta_a \le 600°C$: $$C_a = 425 + 7{,}73\times10^{-1}\theta_a - 1{,}69\times10^{-3}\theta_a{}^2 + 2{,}22\times10^{-6}\theta_a{}^3$$ Eq. (4-18)

$600°C \le \theta_a \le 735°C$: $$C_a = 666 + \frac{13002}{738 - \theta_a}$$ Eq. (4-19)

$735°C \le \theta_a \le 900°C$: $$C_a = 545 + \frac{17820}{\theta_a - 731}$$ Eq. (4-20)

$900°C \le \theta_a \le 1200°C$: $$C_a = 650$$ Eq. (4-21)

Where $T_s$ is the steel temperature [°C]. The graphical variation of this property is represented in Figure 37.

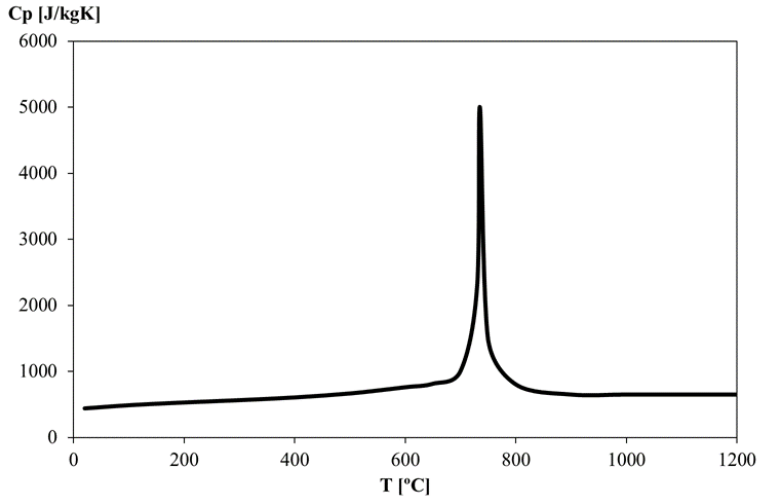


Figure 37: Specific heat of carbon steel as a function of the temperature [4]

#### 4.2.1.2- Thermal Conductivity

The thermal conductivity of steel $\lambda_a$ should be determined according to the following equations, in SI units W/mK.

$20°C \le \theta_a \le 800°C$ $\quad \lambda_a = 54 - 3{,}33 \times 10^{-2} \theta_a$ Eq. (4-22)

$800°C \le \theta_a \le 1200°C$ $\quad \lambda_a = 27{,}3$ Eq. (4-23)

Where $\theta_a$ represents the steel temperature [°C]. The graphical variation of this property is represented in Figure 38.

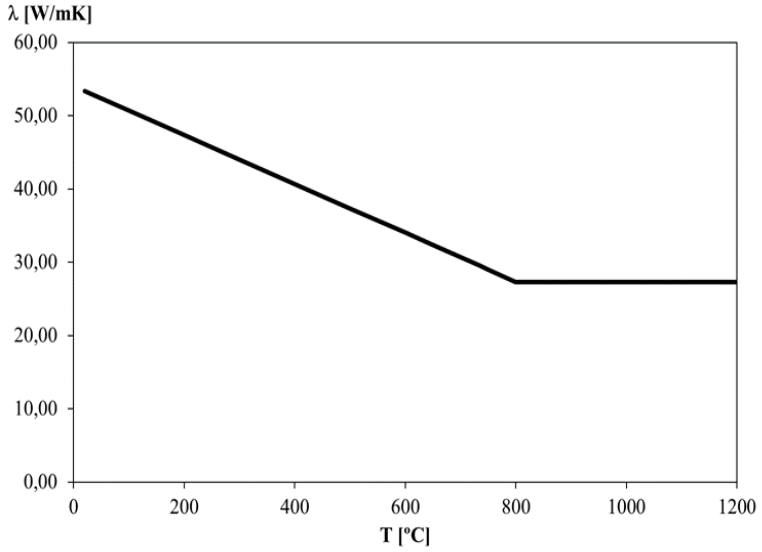


Figure 38: Thermal conductivity of carbon steel as a function of the temperature [4].

### 4.3- The Calculation Method for Unprotected Steel

The Eurocode (EN 1993-1-2) gives a simple equation method for calculating the thermal response of unprotected steel elements. The analytical method, called stepwise, for unprotected steel sections is based on the principle that under fire conditions, the amount of the heat transferred to the surface of the steel member (profile) in the time interval $\Delta t$ (s) is equal to the quantity of energy required to raise the temperature of the steel by $\Delta T_{steel}$ ($^{\circ}C$), assuming that the temperature is uniform over the section of the steel profile element.

$$\dot{h}_{net,d}\, k_{sh} \Delta t = \Delta T_{steel} C_a \rho_a V \; ; \Delta t \le 5s \qquad \text{Eq. (4-24)}$$

Considering a uniform temperature distribution, the increasing of the temperature $\Delta T_{steel}$ during the time interval $\Delta t$ is calculated according to:

$$\Delta T_{steel} = k_{sh} \frac{A_m / V}{C_a . \rho_a} \dot{h}_{net,d} . \Delta t \; ; \Delta t \le 5s \qquad \text{Eq. (4-25)}$$

Where: $k_{sh}$ : is correction factor for the shadow effect, $A_m/V$ is the section factor for unprotected steel members [$m^{-1}$], $A_m$ is the surface area of the member per unit length exposed to fire [$m^2/m$], $V$ is the volume of the member per unit length [$m^3/m$] exposed to fire, $C_a$ is the specific heat of steel [J/kgK], $\rho_a$ is the specific mass of steel [$kg/m^3$], $\dot{h}_{net,d}$ : is the design value of the net heat flux per unit area [$W/m^2$], and finally $\Delta t$ : is the time interval [sec].

An incremental process must be applied to solve the equation, because the specific heat $C_a$ and the net heat flux $\dot{h}_{net,d}$ depend on temperature. A spreadsheet to determine the temperature within the elements was used, according to the incremental process. According to the Eurocode EN1993-1-2 the time interval should be smaller or equal to 5 s.

Table 9: The Spreadsheet calculation of the steel temperature

| Time (s) | Fire Tgas (°C) | Element $T_{steel}$ (°C) | $\dot{h}_{net,d}$ (W/m$^2$) | $C_a$ (J/kgK) | $\Delta\theta_{a,t}$ (°C) | $T_{steel,\ real}$ (°C) |
|---|---|---|---|---|---|---|
| 0 | 20 | 20 | 0 | 440 | 0 | 20 |
| 5 | 33 | 20 | 376 | 440 | 0.05 | 20 |
| 10 | 46 | 20 | 758 | 440 | 0.10 | 20 |
| 15 | 59 | 20 | 1146 | 440 | 0.15 | 20 |
| 20 | 71 | 20 | 1542 | 440 | 0.21 | 21 |
| 25 | 84 | 21 | 1945 | 440 | 0.26 | 21 |
| 30 | 97 | 21 | 2357 | 440 | 0.32 | 21 |
| 35 | 110 | 21 | 2778 | 441 | 0.37 | 21 |
| 40 | 123 | 21 | 3208 | 441 | 0.43 | 22 |
| 240 | 637 | 107 | 39609 | 491 | 4.76 | 111 |
| 960 | 637 | 512 | 15264 | 675 | 1.33 | 513 |
| 1200 | 771 | 604 | 27742 | 765 | 2.14 | 607 |
| 1260 | 789 | 630 | 28021 | 796 | 2.08 | 632 |
| 1440 | 830 | 699 | 26622 | 898 | 1.75 | 701 |
| 1500 | 884 | 723 | 35981 | 939 | 2.26 | 725 |
| 1620 | 805 | 756 | 10234 | 1003 | 0.60 | 757 |
| 1800 | 774 | 768 | 1328 | 1027 | 0.08 | 768 |
| 1920 | 748 | 766 | -3576 | 1024 | -0.21 | 766 |
| 1980 | 732 | 763 | -5922 | 1017 | -0.34 | 763 |
| 2100 | 692 | 751 | -10790 | 993 | -0.64 | 751 |
| 2280 | 570 | 714 | -21287 | 924 | -1.36 | 713 |
| 4200 | 20 | 289 | -10397 | 561 | 0 | 289 |

After using the iterative procedure for the calculation, the temperature evolution of the gas temperature of the steel was determined, see Figure 39.

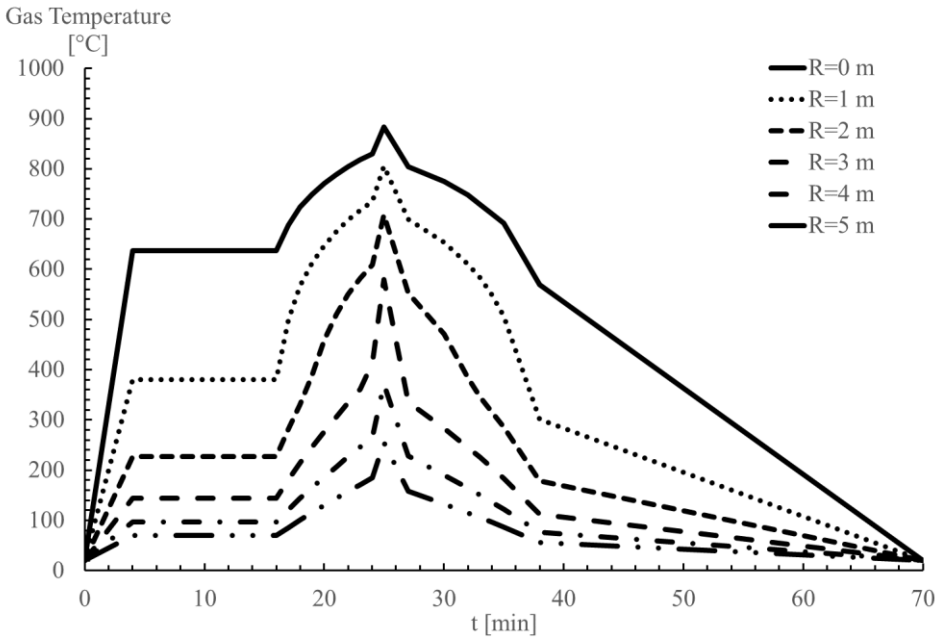


Figure 39: The gas Temperature for the class 03 cars from different position to the beam.

Figure 40 shows the evolution of the gas temperature from different position of the beam to the flame axis. This is the result of a localized fire, using a class 3 car fire source. it can be seen at t=25 min the maximum temperature of the flame is 884 °C, for R=1m the maximum gas temperature is 806 °C, 709°C and 579°C, are the temperature values for R=2m R=3m. The temperature value for R=4m and R=5 m is 372 C and 256°C, respectively.

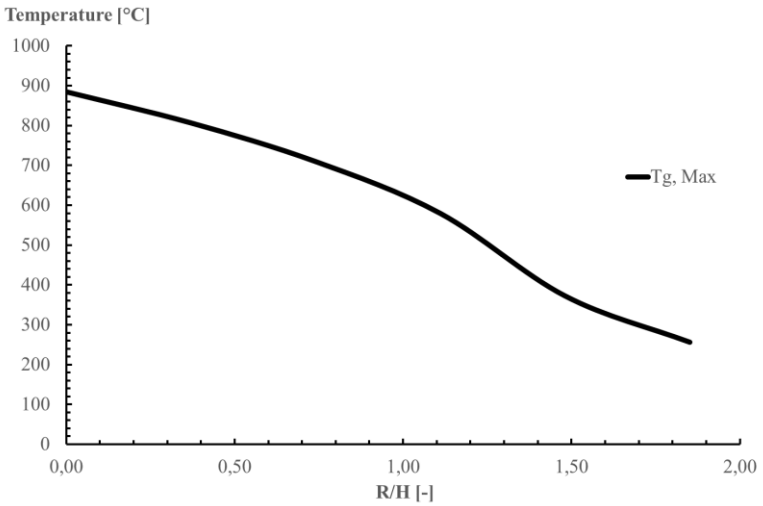


Figure 40: The variation of maximum gas temperature as function of the parameter R.

Figure 41 represents the temperature of the material during the fire event. The maximum temperature is expected to be achieved after the maximum HRR has been reached (25 minutes).

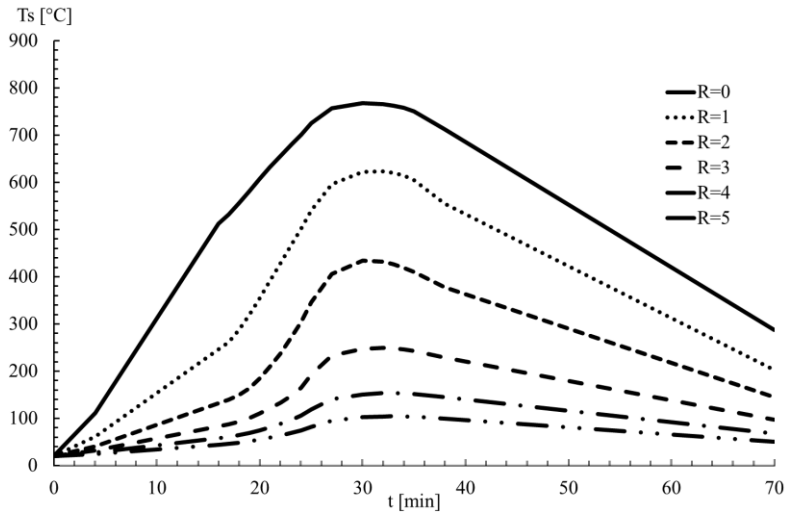


Figure 41: The Temperature of steel beam for different position to the fire axis

The maximum temperature of the materials is achieved for time equal to 32 minutes. For the plume zone the maximum temperature is 768°C. The temperature of steel profile located at 5m from the flume zone axis is 104°C.

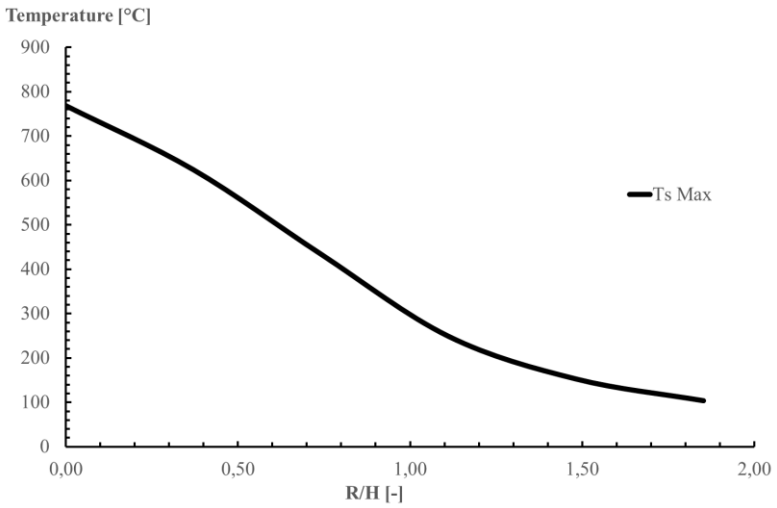


Figure 42: The evolution of the steel temperature as function of the parameter R

This page was intentionally left in blank

# CHAPTER 5: The Software Elefir-EN

## 5.1- Introduction

With the recent approval of the Eurocodes, it became possible for structural engineers to consider the fire assessment based on thermal actions, and based on the performance based design approach, instead of using prescriptive rules based on nominal fire curves. This opens the door to the use of much more realistic fire event scenarios and consequently allowing for more cost effective structures without compromising their safety in case of fire.

The guidance document for construction products L (Directive - 89/106/EEC) gives information about the application and use of Eurocodes. This document states that one of the goal and benefit of the Eurocode programme is that it allows common design aids and software to be developed for use in all Member States. The software Elefire-EN, that is in line with this statement, was used in this work to model the thermal response of the steel beams of an open car park subjected to a localised fire according to Annex C of Part 1-2 of Eurocode 1.

The software allows for the calculation of the critical temperature of the steel members and subsequent evaluation of the thickness of the fire protection material necessary to fulfil the required fire resistance.

The main objective of this work is not to check the fire resistance of a real car park but also to validate the calculation process. This validation is performed with the comparison for the temperature evolution using software Elefir-EN.

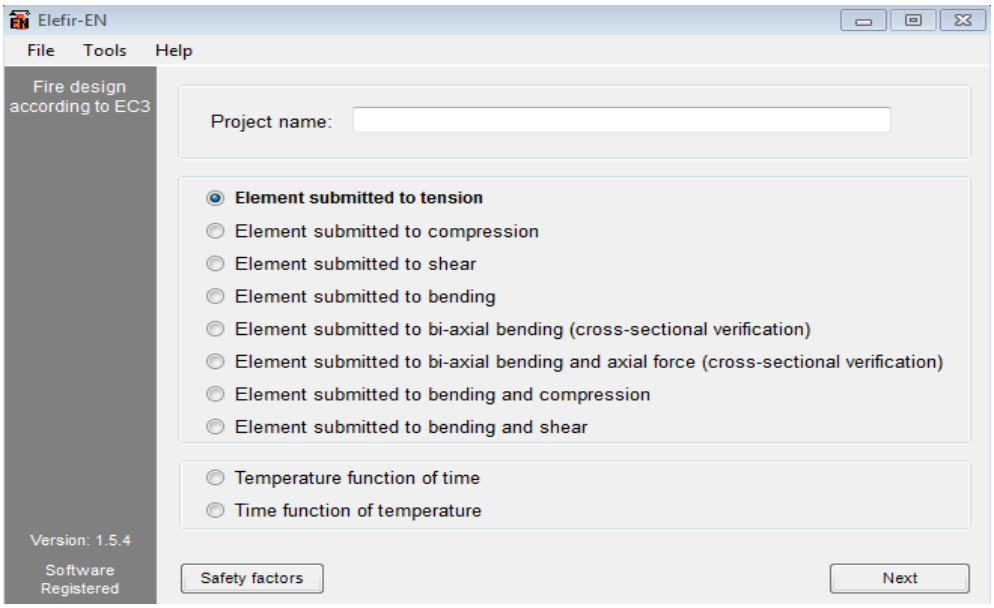


Figure 43: Elefir-EN main menu for different possibilities of mechanical calculations. [12]

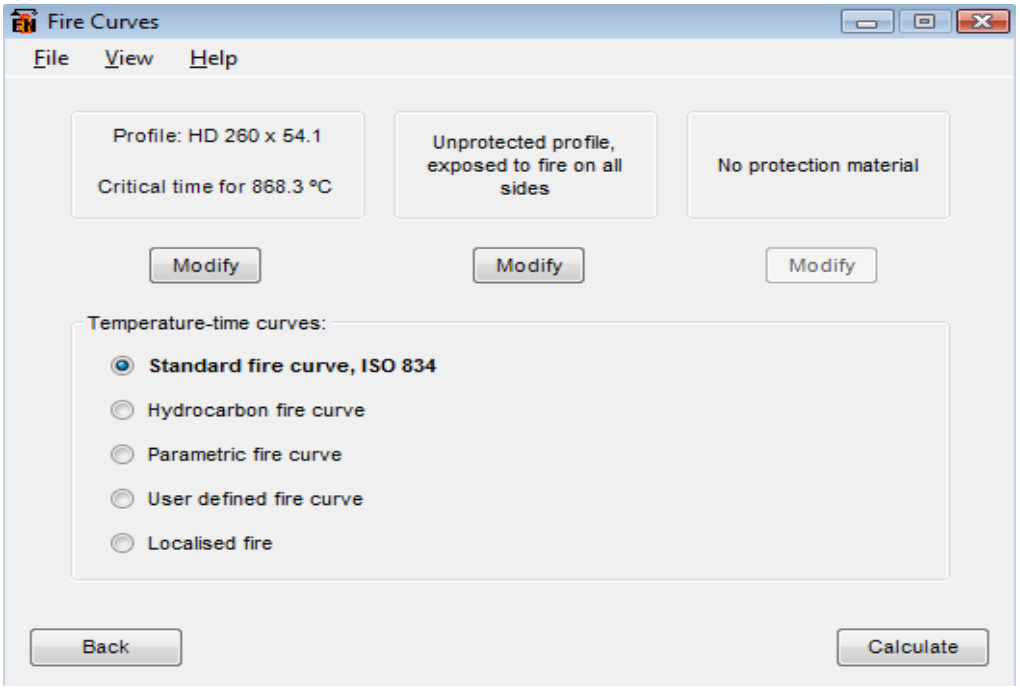


Figure 44: Elefir-EN fire curves for thermal calculations. [12]

## 5.2- Characterization of The Fire

According the European Project "Demonstration of real fire tests in car parks and high buildings" (European Commission, 2001) the classification of cars based on its calorific potential is given in Table 2. These results were obtained using the calorimetric hood to collect all smokes, combustion products and pollutants emitted during the combustion of real car burning. From the tests several experimental curves of the Heat Release Rate (HRR) function of the time were obtained and simplified curves were proposed and validated.

Figure 45 shows the simplified HRR curve for a class 3 car fire. The referred project also suggests curves for the same type of cars that start burning with a delay of 12 and 24 minutes. In Figure 46 these curves are shown and a fourth curve for of a car that starts to burn with a delay of 36 minutes has been added. Table 10 presents the main control points for the definition of each curve.

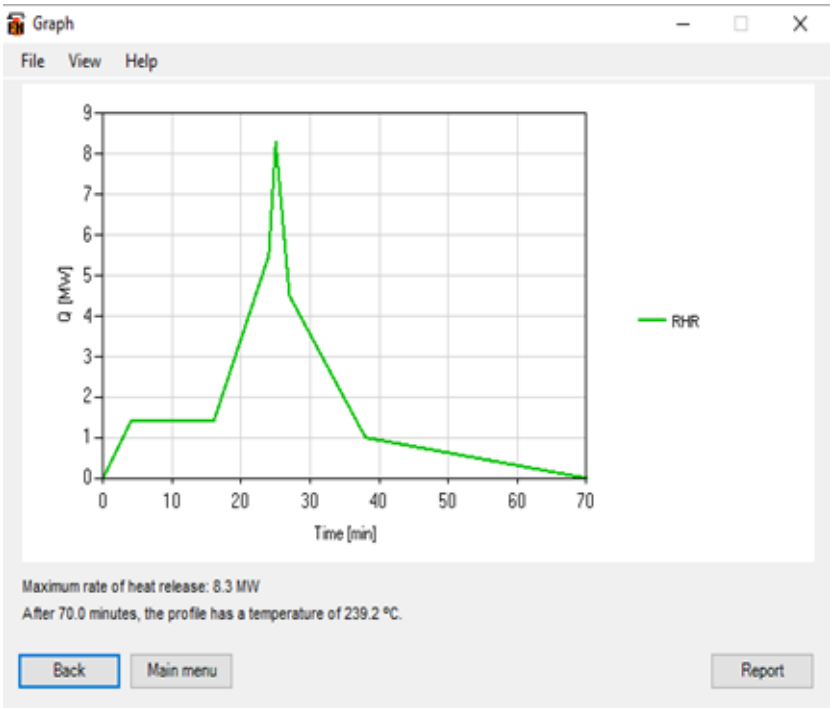


Figure 45: Heat release Rate of a single class3. [12]

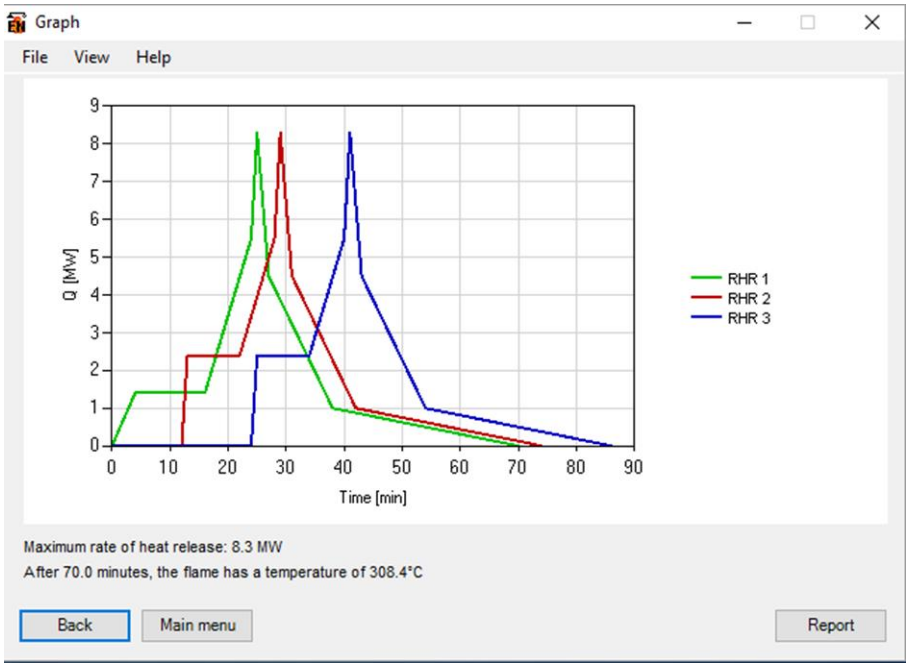


Figure 46: Heat Release Rate of single class 03 with a delay of 12 min. [12]

Table 10: Values of the heat Release Rate of three burning class 3-cars.

| Time (min) | 1st Car | Time (min) | 2nd Car | Time (min) | 3rd Car |
|---|---|---|---|---|---|
| 0 | 0 | 12 | 0 | 24 | 0 |
| 4 | 1.4 | 13 | 2.4 | 25 | 2.4 |
| 16 | 1.4 | 22 | 2.4 | 34 | 2.4 |
| 24 | 5.5 | 28 | 5.5 | 40 | 5.5 |
| 25 | 8.3 | 29 | 8.3 | 41 | 8.3 |
| 27 | 4.5 | 31 | 4.5 | 43 | 4.5 |
| 38 | 1 | 42 | 1 | 54 | 1 |
| 70 | 0 | 74 | 0 | 86 | 0 |

### 5.3- Temperatures of The Beam with Hasemi Model

The program Elefir-EN [12] first evaluates the length of the flame to decide which method has to be used (Heskestad or Hasemi). In the case of multiple localised fires only the fires in which the flame impacts the ceiling are considered and the others are ignored Figure 47 shows the flame length development during the fire, considering that the diameter of the cars is D = 2 m and the distance between the fire level and the compartment is H 2.7 m.

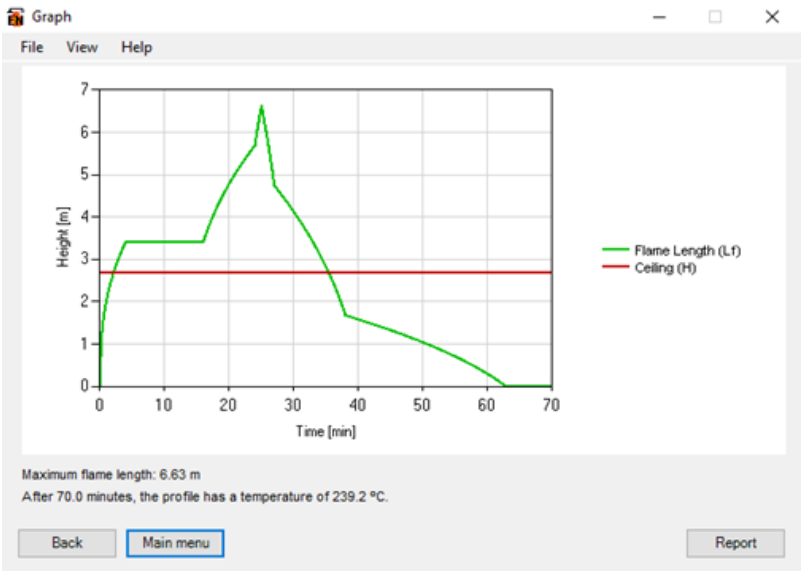


Figure 47: Flame Length development for a single burning car [12]

From Figure 48 to Figure 53 the gas temperature of the fire event for burning a car-class3 and the temperature of the secondary beam are presented for different positions relative to the flame axis (parameter r =0m,1m,…,5m). The secondary beam is made of IPE A 600, the maximum temperature is 758 ºC

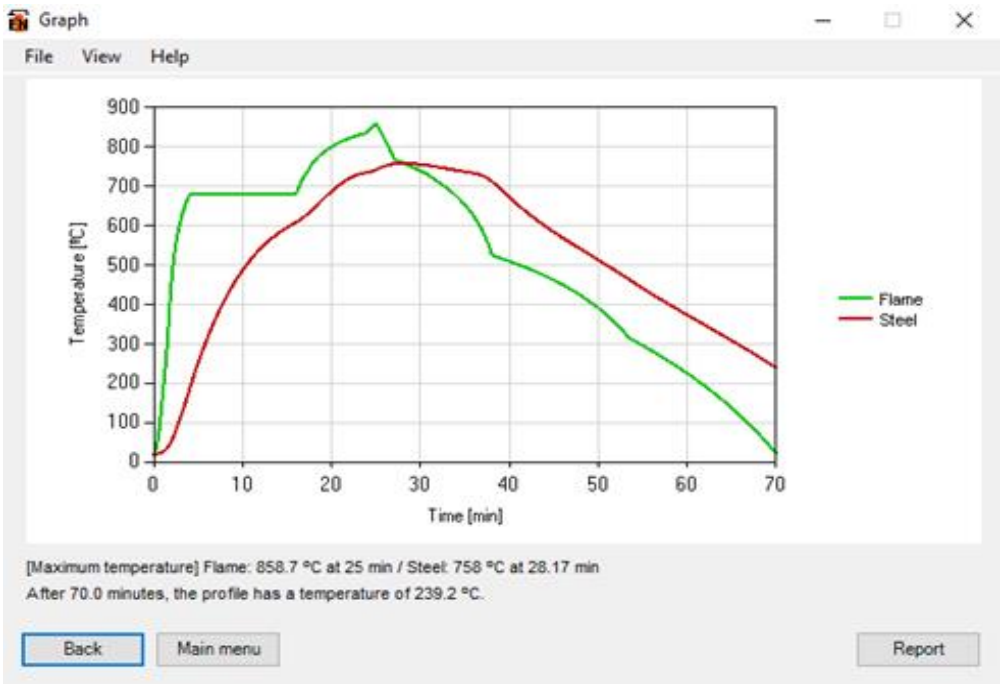


Figure 48: Flame and steel temperature of R=0m from the fire axis. [12]

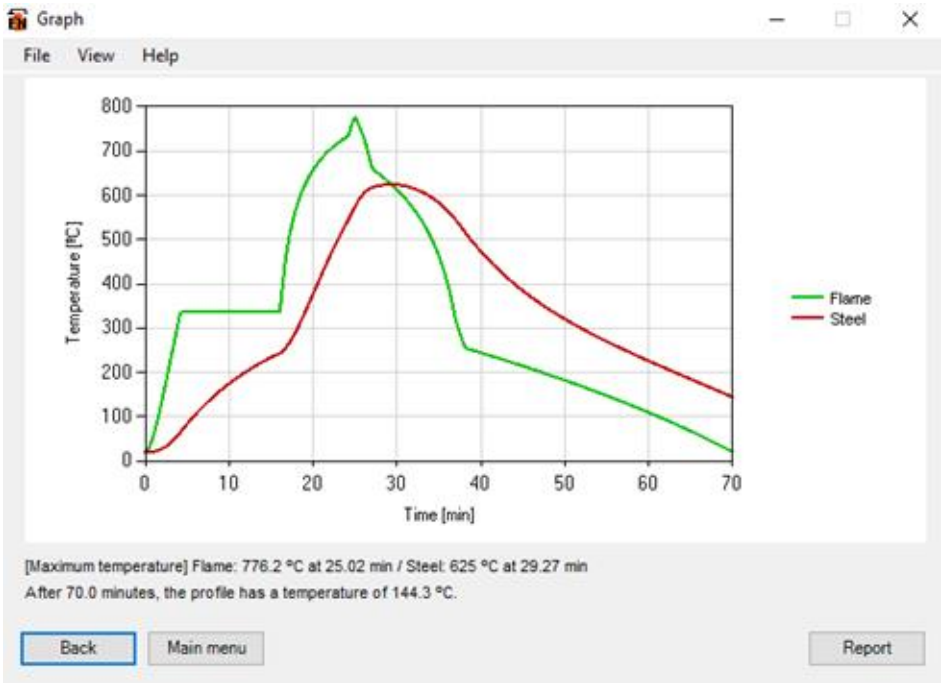


Figure 49: Flame and steel temperature of R= 1m from the fire axis. [12]

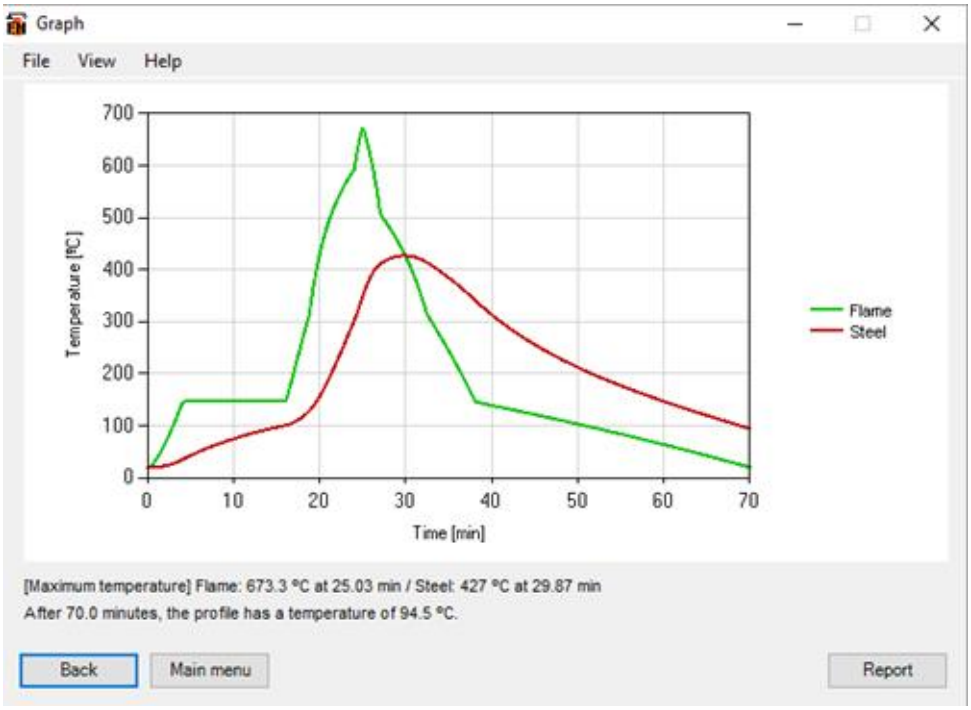


Figure 50: Flame and steel temperature of R=2m from the fire axis. [12]

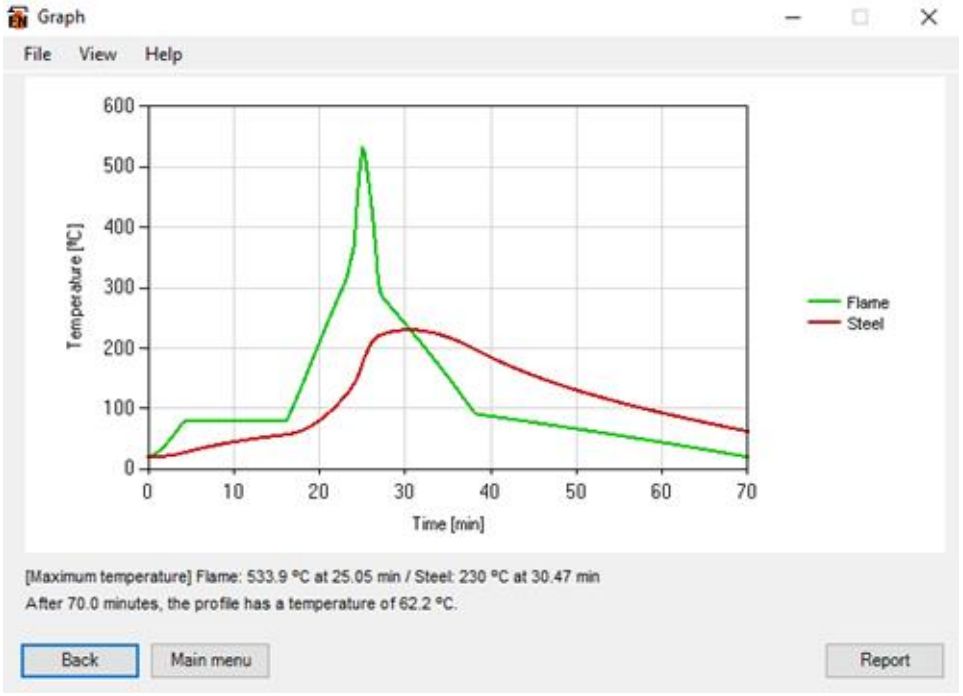


Figure 51: Flame and steel temperature of R=3m from the fire axis. [12]

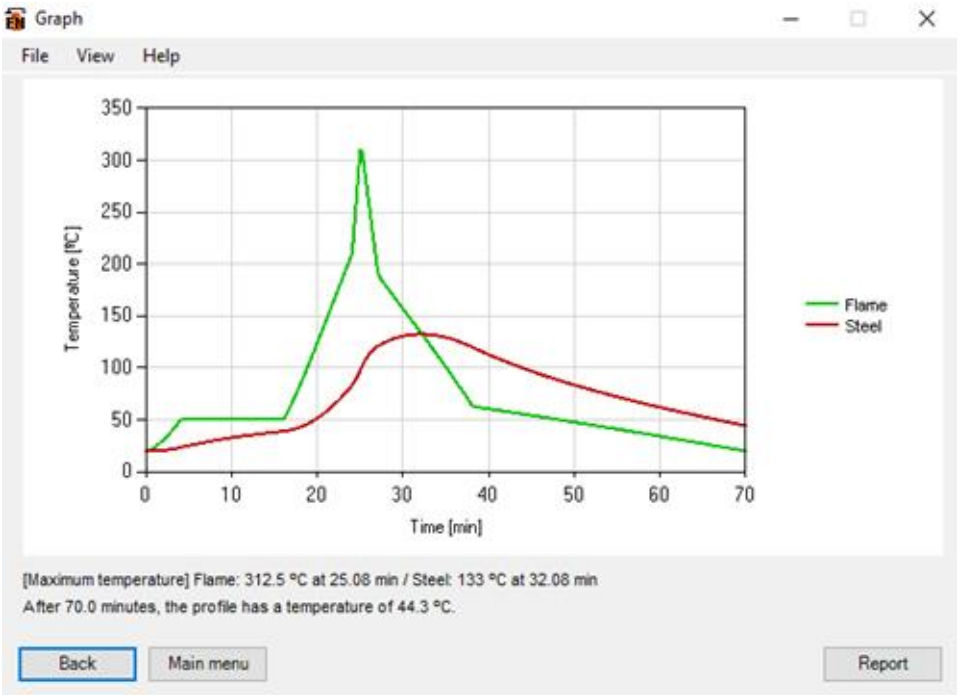


Figure 52: Flame and steel temperature of R=4m from the fire axis. [12]

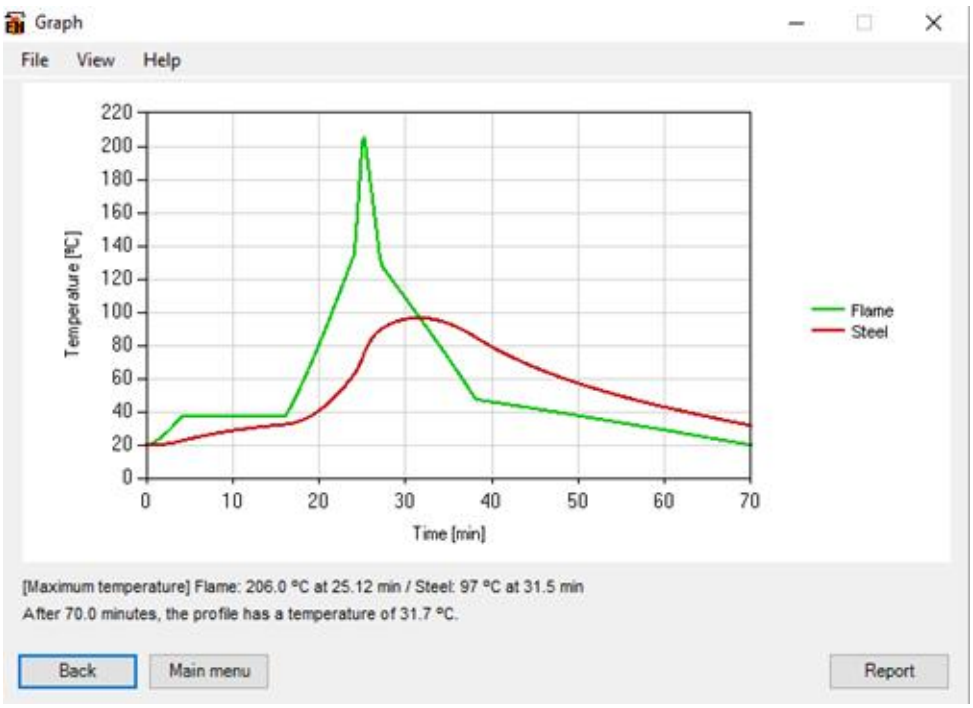


Figure 53: Flame and steel temperature of R=5m from the fire axis. [12]

Table 10 shows both of the maximum gas temperature and the maximum temperature obtained for the secondary beam in different radial positions to the axis of flame or plume zone.

From this table it can be concluded that, due to the scenario 1 the secondary beams should be protected so that the temperature doesn't reach the assumed critical temperature of

560 ºC [34] during the complete duration of the fire including the cooling phase or during a required period of time.

Table 11:The critical Gas and steel temperature of the profile IPE A 600.

| | R = 0m | R = 1m | R = 2m | R = 3m | R = 4m | R = 5m |
|---|---|---|---|---|---|---|
| $\theta_{steel}$, max °C | 758 | 625 | 427 | 230 | 133 | 97 |
| $\theta_{gas}$, max °C | 859 | 776 | 673 | 534 | 313 | 206 |

### 5.4- Comparison of Results

#### 5.4.1- The Comparison of Class 1

Figure 54 shows the variation of the both gas and steel temperature as function of time, during the fire event of class 1 for R=0 m from the fire plume. The results obtained from the simplified method give: maximum temperature of gas is 824°C after 25 min of fire, the steel profile reaches a maximum temperature of 673°C determined after 32 min from the beginning of the fire.

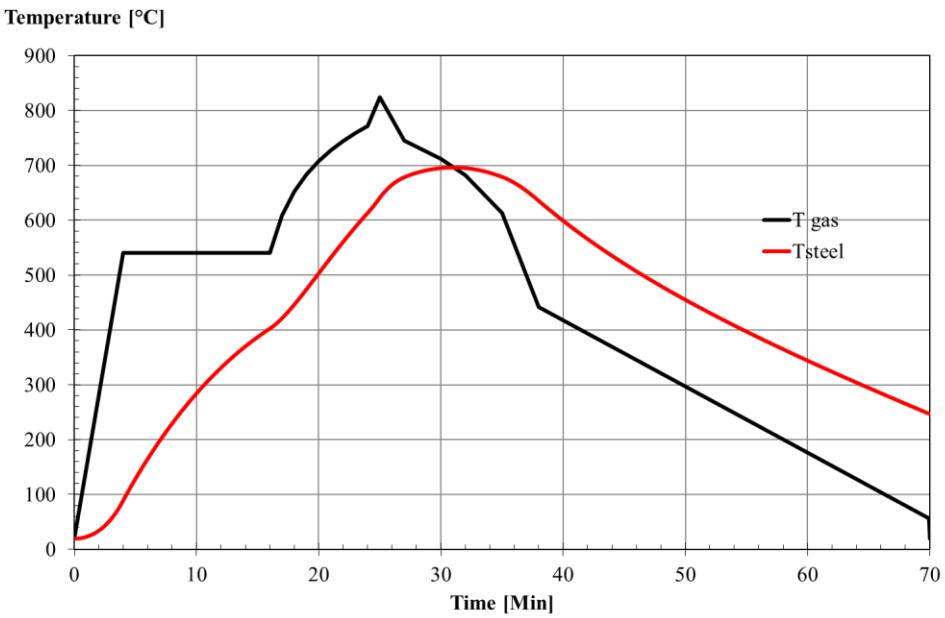


Figure 54: Gas and steel temperature evolution for class 1 of cars with R=0m

Figure 55 shows the comparison between the simplified method and Elefir-EN software. Differences are identified for the gas and steel temperature curves, due to the class 1

fire event. The results were calculated for the radial position R=0. Next table shows the relative error for comparison.

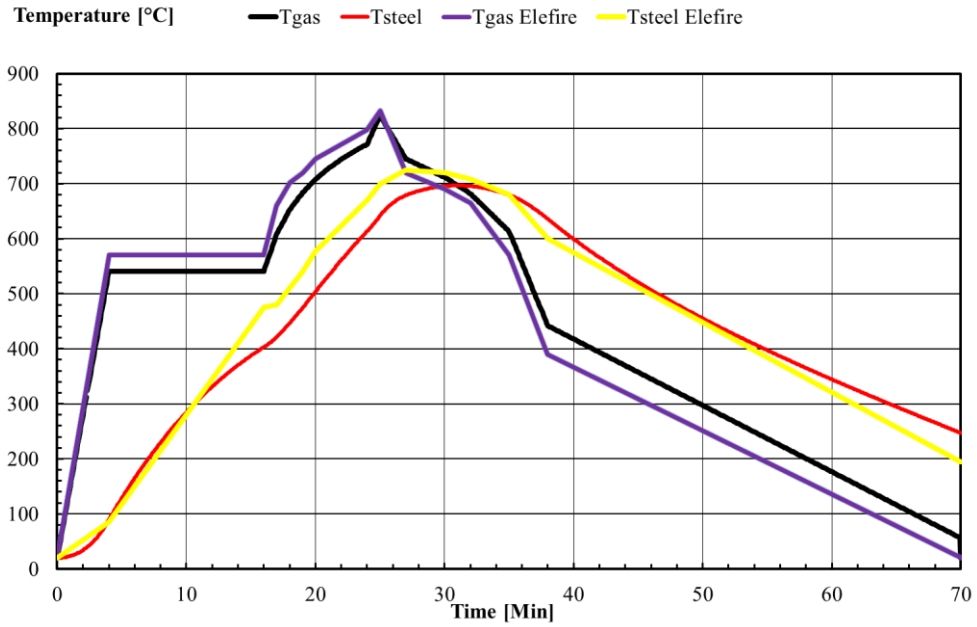


Figure 55: The class 1 comparison between excel and Elefir-EN software.

Table 12: The relative Error of Comparison for cars from class 1.

| | EXCEL | | ELIFIR | | Relative errer | Relative errer |
|---|---|---|---|---|---|---|
| **TIME** | **Tgas** | **Tmat** | **Tgas** | **Tmat** | **Tgas** | **Tsteel** |
| Min | °C | °C | °C | °C | °C | °C |
| 0 | 20 | 20 | 20 | 20 | **0,00** | **0,00** |
| 4 | 541 | 90 | 570 | 85 | **-0,05** | **0,05** |
| 16 | 541 | 403 | 570 | 475 | **-0,05** | **-0,15** |
| 17 | 609 | 422 | 660 | 480 | **-0,08** | **-0,12** |
| 18 | 652 | 447 | 702 | 510 | **-0,07** | **-0,12** |
| 19 | 684 | 475 | 720 | 540 | **-0,05** | **-0,12** |
| 20 | 708 | 504 | 745 | 577 | **-0,05** | **-0,13** |
| 24 | 772 | 614 | 798 | 670 | **-0,03** | **-0,08** |
| 25 | 824 | 641 | 833 | 699 | **-0,01** | **-0,08** |
| 27 | 745 | 679 | 720 | 724 | **0,03** | **-0,06** |
| 30 | 712 | 695 | 690 | 720 | **0,03** | **-0,03** |
| 32 | 682 | 696 | 665 | 708 | **0,03** | **-0,02** |
| 35 | 613 | 680 | 570 | 680 | **0,08** | **0,00** |
| 38 | 442 | 636 | 390 | 600 | **0,13** | **0,06** |
| 70 | 20 | 20 | 20 | 20 | **0,00** | **0.00** |

### 5.4.2- The Comparison of Class 2

Figure 56 shows the variation of the both gas and steel temperature as function of time, during the fire event of class 2 for the radial position R=0 m from the plume. The results obtained from the simplified method give: maximum temperature of gas is 853°C after 25 min

of fire, the steel profile reaches a maximum temperature of 733°C determined after 30 min from the beginning of the fire.

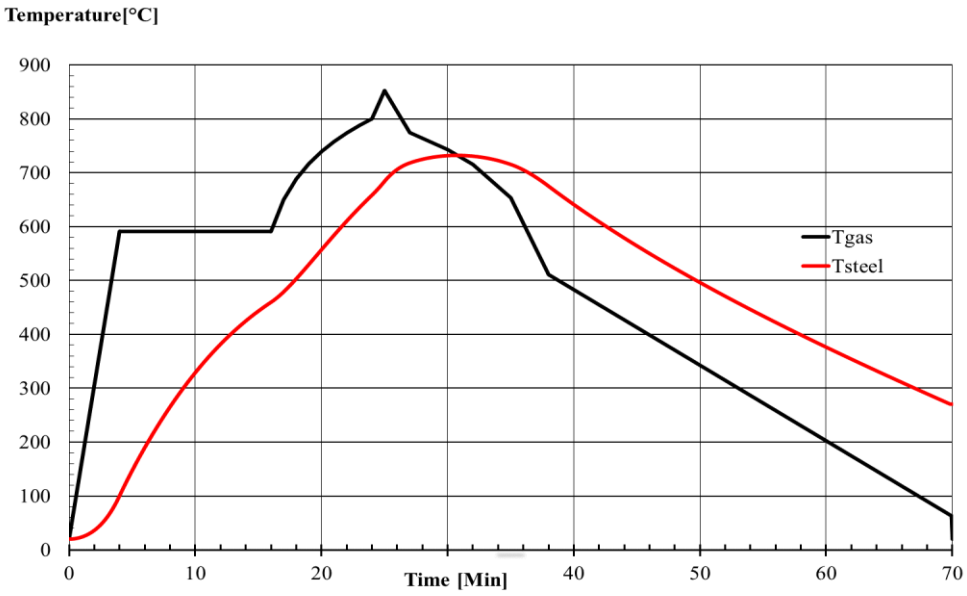


Figure 56: Gas and steel temperature evolution for class 2 of cars with R=0m

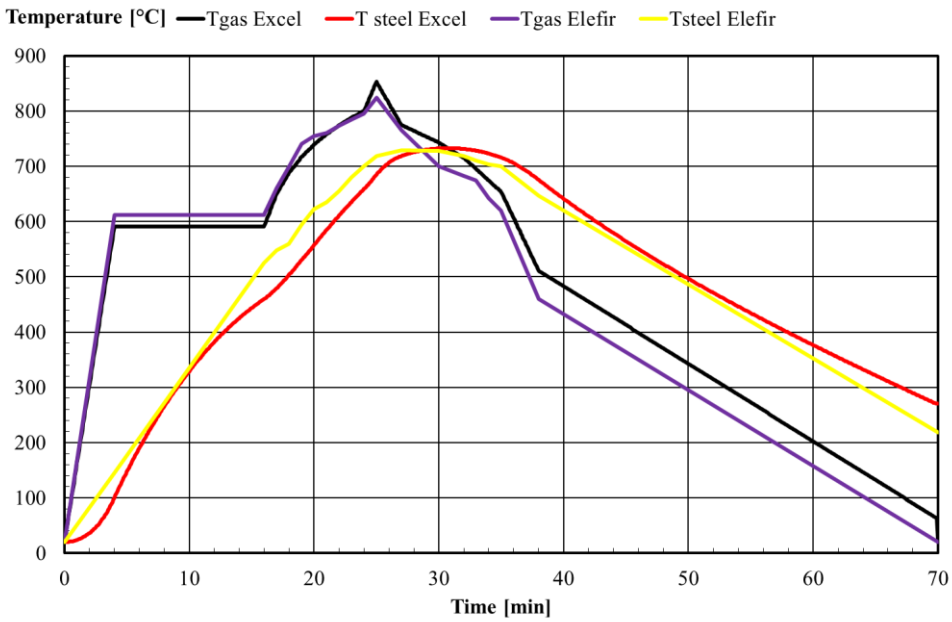


Figure 57: The class 2 cars comparison between excel and Elefir-EN software.

Figure 57 shows the comparison between the simplified method and Elefir-EN software Differences are identified for the gas and steel temperature curves, due to the class 2 fire event. The results were calculated for the radial position n R=0. Next table shows the relative error for comparison.

Table 13: The relative Error of Comparison for cars from class 2.

| Time Min | Time Sec | Excel Tgas °C | Tsteel °C | Elefir-EN Tgas °C | Tsteel °C | Relative Error Tgas °C | Relative Error Tsteel °C |
|---|---|---|---|---|---|---|---|
| 0 | 0 | 20 | 20 | 20 | 20 | **0,00** | **0,00** |
| 4 | 240 | 591 | 103 | 612 | 145 | **-0,03** | **-0,25** |
| 16 | 960 | 591 | 471 | 612 | 525 | **-0,03** | **-0,10** |
| 20 | 1200 | 739 | 559 | 755 | 622 | **-0,02** | **-0,10** |
| 24 | 1440 | 800 | 660 | 795 | 700 | **0,01** | **-0,06** |
| 25 | 1500 | 853 | 685 | 824 | 718 | **0,03** | **-0,05** |
| 27 | 1620 | 775 | 719 | 765 | 729 | **0,01** | **-0,01** |
| 30 | 1800 | 743 | 733 | 700 | 728 | **0,06** | **0,01** |
| 32 | 1920 | 715 | 731 | 682 | 718 | **0,05** | **0,02** |
| 33 | 1980 | 695 | 728 | 675 | 710 | **0,03** | **0,03** |
| 34 | 2040 | 674 | 723 | 642 | 704 | **0,05** | **0,03** |
| 35 | 2100 | 654 | 716 | 620 | 700 | **0,05** | **0,02** |
| 38 | 2280 | 511 | 676 | 460 | 647 | **0,11** | **0,04** |
| 70 | 4200 | 20 | 271 | 20 | 20 | **0,00** | **0,00** |

### 5.4.3- The Comparison of Class 3

Figure 58 shows the variation of the both gas and steel temperature, calculated by this method. as function of time for radial position R=0 m from the fire axis. The maximum temperature for gas is 884°C after 25 min of fire. The steel profile has a maximum temperature of 725°C achieved for time equal to 32 min.

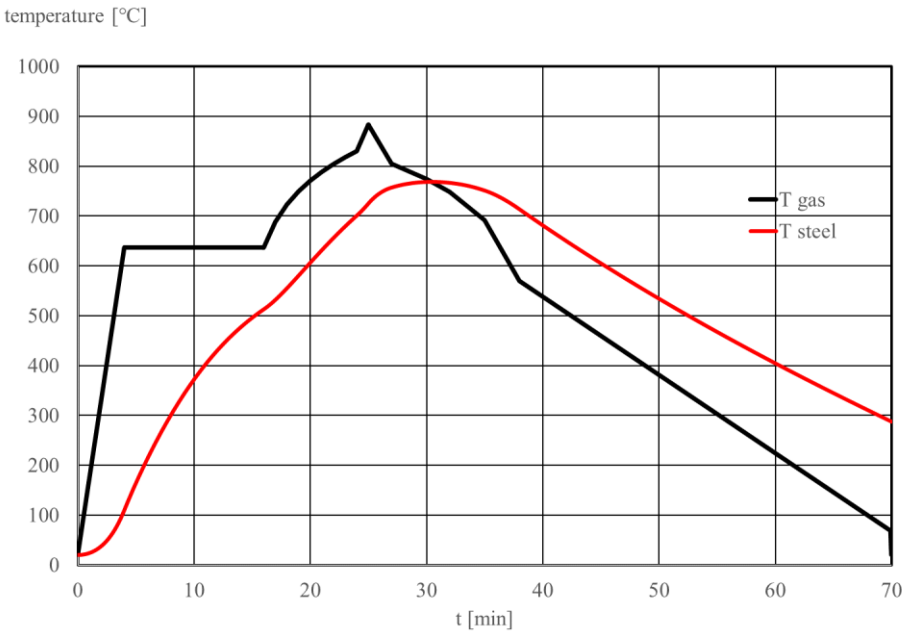


Figure 58: Gas and steel temperature evolution for class 3 of cars with R=0m.

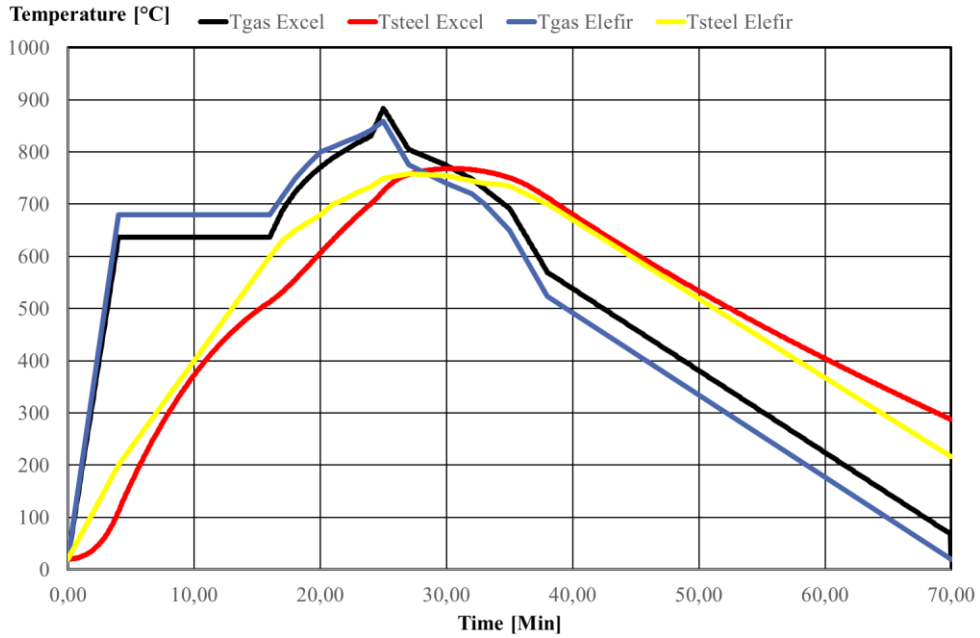


Figure 59: The class 3 comparison between excel and Elefir-EN software.

Figure 59 shows the comparison between the results obtained by the simplified method and software Elefire-EN. The comparison between results is presented in the next table.

Table 14: The relative Error of comparison for cars from class 3.

| | | Excel | | Elefir-EN | | Relative error | Relative error |
|---|---|---|---|---|---|---|---|
| **Time** | **Time** | **Tgas** | **Tsteel** | **Tgas** | **Tsteel** | **Tgas** | **Tsteel** |
| Min | sec | °C | °C | °C | °C | | |
| 0 | 0 | 20 | 20 | 20 | 20 | **0,00** | **0,00** |
| 4 | 240 | 637 | 111 | 680 | 200 | **-0,06** | **-0,35** |
| 16 | 960 | 637 | 513 | 680 | 600 | **-0,06** | **-0,15** |
| 20 | 1200 | 771 | 607 | 800 | 680 | **-0,04** | **-0,11** |
| 24 | 1440 | 830 | 701 | 842 | 734 | **-0,01** | **-0,05** |
| 25 | 1500 | 884 | 725 | 859 | 749 | **0,03** | **-0,03** |
| 27 | 1620 | 805 | 757 | 775 | 758 | **0,04** | **0,00** |
| 30 | 1800 | 774 | 768 | 740 | 755 | **0,05** | **0,02** |
| 32 | 1920 | 748 | 766 | 720 | 745 | **0,04** | **0,03** |
| 33 | 1980 | 729 | 763 | 700 | 740 | **0,04** | **0,03** |
| 34 | 2040 | 710 | 758 | 675 | 739 | **0,05** | **0,03** |
| 35 | 2100 | 692 | 751 | 650 | 735 | **0,06** | **0,02** |
| 38 | 2280 | 570 | 713 | 523 | 700 | **0,09** | **0,02** |
| 70 | 4200 | 20 | 287 | 20 | 217 | **0,00** | **0,29** |

### 5.4.4- The Comparison of Class 4-5

Figure 60 shows the variation of the both gas and steel temperature as function of time, during the fire event of class 4 or 5 for the radial position R=0 m from the plume. The results obtained from the simplified method give: maximum temperature of gas is 911°C after 25 min

of fire, the steel profile reaches a maximum temperature of 792°C determined after 30 min from the beginning of the fire.

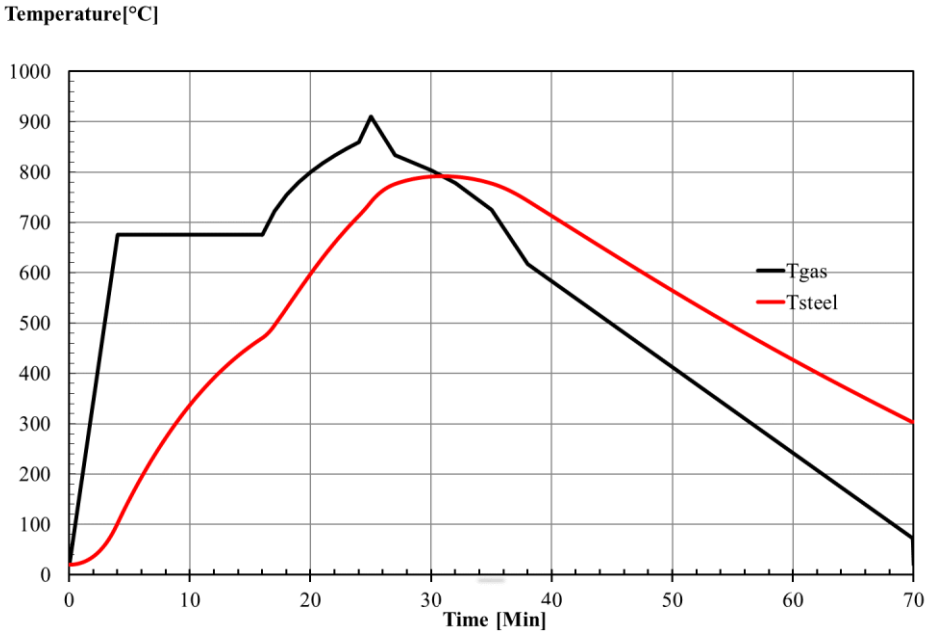


Figure 60: Gas and steel temperature evolution for class 4-5 of cars with R=0m

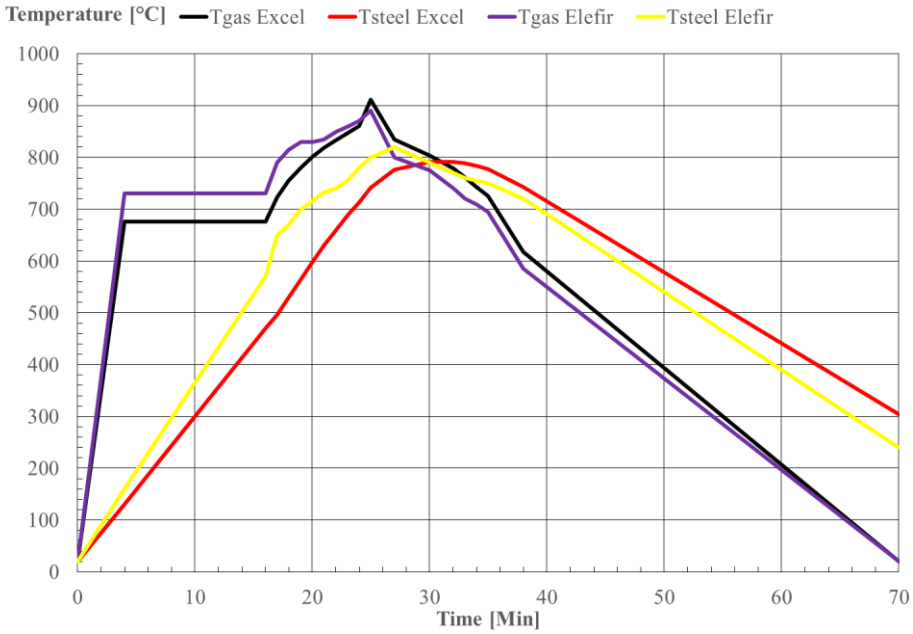


Figure 61: The class 4-5 cars comparison between excel and Elefir-EN software

Figure 61 shows the comparison between the simplified method and Elefir-EN software. Differences are identified for the gas and steel temperature curves, due to the class 4

and 5 fire event. The results were calculated for the radial position R=0. Next table shows the relative error for comparison.

Table 15: The relative Error of comparison for cars from class 4-5.

| **Time** Min | **Time** sec | **Excel Tgas** °C | **Tmat** °C | **Elefir Tgas** °C | **Tmat** °C | **Relative error Tgas** °C | **Relative Eroor Tmat** °C |
|---|---|---|---|---|---|---|---|
| 0 | 0 | 20 | 20 | 20 | 20 | **0,00** | **0,00** |
| 4 | 240 | 676 | 130 | 730 | 160 | **-0,07** | **-0,19** |
| 16 | 960 | 676 | 471 | 730 | 570 | **-0,07** | **-0,17** |
| 20 | 1200 | 801 | 598 | 830 | 715 | **-0,04** | **-0,16** |
| 21 | 1260 | 818 | 630 | 835 | 733 | **-0,02** | **-0,14** |
| 22 | 1320 | 834 | 660 | 850 | 740 | **-0,02** | **-0,11** |
| 23 | 1380 | 848 | 688 | 860 | 755 | **-0,01** | **-0,09** |
| 24 | 1440 | 860 | 714 | 870 | 780 | **-0,01** | **-0,09** |
| 25 | 1500 | 911 | 741 | 890 | 800 | **0,02** | **-0,07** |
| 27 | 1620 | 834 | 777 | 800 | 820 | **0,04** | **-0,05** |
| 30 | 1800 | 804 | 792 | 775 | 790 | **0,04** | **0,00** |
| 32 | 1920 | 779 | 791 | 740 | 770 | **0,05** | **0,03** |
| 33 | 1980 | 761 | 789 | 720 | 760 | **0,06** | **0,04** |
| 34 | 2040 | 743 | 784 | 710 | 755 | **0,05** | **0,04** |
| 35 | 2100 | 726 | 778 | 695 | 750 | **0,04** | **0,04** |
| 38 | 2280 | 618 | 743 | 585 | 720 | **0,06** | **0,03** |
| 70 | 4200 | 20 | 304 | 20 | 240 | **0,00** | **0,27** |

# CHAPTER 6: CONCLUSIONS AND FUTURE DEVELOPMENTS

The fire design of steel and composite structures from open car park can be made in accordance with Eurocodes, while Annex C of Eurocode 1992 Part 1.2 [3] present a simplified method for determining the flame temperature around the beams. The calculation of these temperatures depends on the heat release rate (HRR) for each type of car, which is determined based on the fire scenarios. The reference curves for the HRR was defined based on results of experimental tests performed on actual vehicles. Finally, Eurocodes 3 [4] and 4, Part 1.2 [29] present the calculation models for these structures.

From previous experimental tests in real open car park buildings, it was concluded that most of unprotected steel open sided steel-framed car parks have sufficient inherent resistance to withstand the effects of any fires that are likely to occur. These results have encouraged to change the legislations in several European countries, allowing to build steel or composite steel-concrete open car parks without fire protection, taking into account a design based on the actual performance of the structure.

The simplified design methods defined in Eurocodes 3 and 4, part 1.2, are based on conservative assumptions and only allow the use of nominal temperature-time curves for the design of individual members. When the structure is subject to natural fire defined by the HRR fire curves, the choice must involve the use of advanced calculation methods rather than simplified methods in order to consider the indirect effects due to restrained thermal expansions.

The design of columns under localized fires can be done using advanced models. No accurate simple method is available to calculate the column temperature due to a localized fire. Hasemi´s method is a simple tool for the evaluation of the localized effect of a fire on horizontal elements located above the fire, but cannot be used for the columns. [35].

Finally, the examples clearly showed the advantage of using the design methodology based on fire scenarios against the use of ISO curve. It was verified that the unprotected composite steel-concrete structure resists to fire when using different fire events.

In conclusion, the design methodology based on fire scenarios allowed optimizing the structure to benefit from an appropriate level of fire safety, reducing the fire protection and therefore the final cost of this type of building.

The current simplified method was implemented to calculate the temperature of the gas and the temperature of the beam element, using different relative positions between the fire source and the position of the steel element.

Future developments are proposed to continue this study: A CFD comparison should be performed to account for the effect of fire dynamics on this kind of events. An experimental study can be performed in a small scale to validate the numerical simulation.

## REFERENCES


[1] Fraud, C., Zhao, B., Joyeux, D., Kruppa, J., "*Guide Pour la Vérification du Comportement au Feu de Parcs de Stationnement Large Ment ventilés en Superstructure Métallique*", CTICM, INSI – 03/233d – BZ/PB, 2004, page 75.

[2] Schleich J.B, chainnan, L.G. Cajot, secretary, J.P. Bouillette, P. Loikkanen, F. Münzker, E. Pedersen, *Fire Safety in Open Car Parks-Modern Fire Engineering*, Chairman of the ECCS-Technical Committee 3, Bem, August 1993, page 33-43.

[3] CEN, *Eurocode 2 - Design of steel structure part 1.2: General rules. Structural fire design*. Brussels, December 2004.

[4] Eurocode 3: Design of steel structures. Part 1.2: General rules. Structural fire design. Draft ENV 1993-1-2, CEN, Brussels, may 1995.

[5] ArcelorMittal, 2007 "*Parkings aériens métalliques largement ventilés*". Les carnets de l'acier No 9, New Edition, 2007 (in French).

[6] Salvatore Vaccaro, Maria Grazia Meo, "*Modelling of Enclosure Fires*", Department of Chemical and Food Engineering Ph.D. Course in Chemical Engineering (VII Cycle-New Series), 2006, page 5-10.

[7] Gobeau, N., Ledin, H.S. and Lea, C.J. (2002) "*Guidance for HSE Inspectors Smoke movement in complex enclosed spaces*", Assessment of Computational Fluid Dynamics. HSL Report HSL, 2002, page 29.

[8] Wen, J. (1996), "*Numerical modelling as a practical aid for the development of smoke control strategies in buildings"*. PhD thesis, University of Kingston (UK).

[9] Bakar, M.Z.A. (1999), "*A study of the effect of tunnel aspect ratio on control of smoke flow in tunnel fires*". PhD thesis, University of Sheffield (UK).

[10] Pope, N. (2005), "*Computational Fluid Dynamics modelling of large-scale compartment fires"*. PhD thesis, University of Manchester (UK).

[11] Hart, R.A. (2005), *"Numerical modelling of tunnel fires and water mist suppression"*. PhD thesis, University of Nottingham (UK).

[12] Vila Real, P., Franssen, J. M., Elefir-EN V1.2.3, *Software for fire design of steel structural members according the Eurocode 3*, 2010. http://elefiren.web.ua.pt.

[13] Leander Noordijk, Tony Lemaire, "*Modelling of fire spread in car parks*", TNO Centre for Fire Research, Delft, the Netherlands, page 1-2, HERON, Vol. 50, No 4 (2005).

[14] E. Annerel, L.Taerwe , B.Merci , D.Jansen , P.Bamonte , R.Felicetti, *Thermo-mechanical analysis of an underground car park structure exposed to fire*, International Association for Fire Safety Science Fire Safety Journal 2013, page 97-98.

[15] Feijter M.P., *Kort verslag brandonderzoek Parkeergarage Ruitersweg* 77, Hilversum, Efectis Nederland, 15 November 2007.

[16] Lemmers, A.C.J.T.B., *Onderzoek schade door brand in parkeergarage appartement en complex*, Dr.Nolenshof te Geleen. Intron, page 23-24, 10 August 2007.

[17] Gemeente Haarlemmermeer, *Onderzoeksrapportage parkeergarage brand Schiphol*, gemeente Haarlemmermeer, 2002.

[18] Cwiklinski, C., *"Parcs de Stationnement en Superstructure Large Ment ventilés – Avis D'expert sur les scénarios d'incendie*", Rapport final, INERIS DRA-CCw/ MCh-2001-cgr22984, 2001, page 26.

[19] Feijter M.P., *Kort verslag brandonderzoek Parkeergarage Schoolstraat*, Hilversum, Efectis Nederland, 29 November 2007.

[20] ECCS, "*Fire Safety in Open Car Parks"*, Modern Fire Engineering, Technical Committee 3, nº75, European Convention for Constructional Steelwork: Brussels, Belgium, 1993, page 90.

[21 Royal Decree establishing the measures for prevention against fire and explosion which closed car parks must meet for the parking of LPG vehicles, Moniteur Belge, Ed. 3, 20 of June, 2007.

[22] Decree of 9 May 2006 approving provisions supplementing and amending the safety regulation against the risks of fire and panic in public buildings (open car parks), Ministry of the Interior and Spatial Planning, Official Journal of the French Republic, July 8, 2006.

[23] Ministry of Interior (Italian Government), Decree 9 May 2007. Guidelines for the implementation of 'fire safety engineering approach, 2007.

[24] Nigro, E., Cefarelli, G., Ferraro, A., Manfredi, G. and Cosenza, E., *"Fire Safety Engineering for Open and Closed Car Parks: C.A.S.E Project for L'Aquila"*, Applied Mechanics and Materials, Vol. 82, pp. 746-751, 2011. ISSN: 1662-7482. doi:10.4028/www.scientific.net/AMM.82.746.

[25] ArcelorMittal "*Car parks in steel*", Comercial Sections, 1996, page 30.

[26] Portaria nº1532/2008", Diário da República, 1ª série, N.º 250, 29 de Dezembro, 2008, page 9050-9127.

[27] Decreto-Lei nº220/2008, Diário da República, 1ª série, N.º 220, 2008, page 7903-7922.

[28] ArcelorMittal 2011, Building Research Institute (ITB), *"Design Guide-Open Steel Car Parks Design for the Polish Market"*, ArcelorMittal Construction Poznan University of Technology, page 20, 2011.

[29] Joyeux et al., 2002 - Joyeux, D., Kruppa J., Cajot L.G., Schleich J.B., van de Leur P., Twilt L. *"Demonstration of real fire tests in car parks and high buildings"*. European

Commission, Contract no 7215-PP/025, CTICM, Final Report, EUR 20466 EN, 2002, page 53-59.

[30] Li, Y. "*Assessement of Vehicle Fires in New Zealand Parking Buildings"*. Fire Engineering Research Report 04/2, Master Thesis, University of Canterbury, New Zealand, May 2004.

[31] Mangs, J. and Keski-Rahkonen, O., *"Characterisation of the Fire Behaviour of a Burning Passenger Car. Part I: Car Fire Experiments."* Fire Safety Journal, 1994, Vol. 23, page. 17-35.

[32] Schleich, J.-B., Cajot, L.-G., Pierre, M., Brasseur, M., Franssen, J.-M. and Kruppa, J. et al., *"Development of Design Rules for Steel Structures Subjected to Natural Fires in Closed Car Parks"*, European Commission, C.E.C. Research 7210-SA/518. Final Report EUR 18867 EN, 1999, page. 154.

[33] J-F. Cadorin, D. Pintea, J-C. Dotreppe, J-M. Franssen, "A tool to design steel elements submitted to compartment fires", OZone V2, Part 2: Methodology and application,2009, page 6-9.

[34] ZHAO Bin, Workshop 'Structural Fire Design of Buildings according to the Eurocodes' – Brussels, 27-28 November 2012.

[35] C. Haremza, A. Santiago and L. Simões da Silva," Design *of Steel and Composite Open Car Parks Under Fire"*, Advanced Steel Construction Vol. 9, No. 4, 23 January 2013, Portugal, page 321-339.